

Serveur Académique Lausannois SERVAL serval.unil.ch

Author Manuscript

Faculty of Biology and Medicine Publication

This paper has been peer-reviewed but does not include the final publisher proof-corrections or journal pagination.

Published in final edited form as:

Title: Mammalian Innate Immune Response to a Leishmania-Resident RNA Virus Increases Macrophage Survival to Promote Parasite Persistence.

Authors: Eren RO, Reverte M, Rossi M, Hartley MA, Castiglioni P, Prevel F, Martin R, Desponds C, Lye LF, Drexler SK, Reith W, Beverley SM, Ronet C, Fasel N

Journal: Cell host & microbe

Year: 2016 Sep 14

Volume: 20

Issue: 3

Pages: 318-28

DOI: [10.1016/j.chom.2016.08.001](https://doi.org/10.1016/j.chom.2016.08.001)

In the absence of a copyright statement, users should assume that standard copyright protection applies, unless the article contains an explicit statement to the contrary. In case of doubt, contact the journal publisher to verify the copyright status of an article.

Mammalian innate immune response to a *Leishmania*-resident RNA virus increases macrophage survival to promote parasite persistence

Remzi Onur Eren¹, Marta Reverté¹, Matteo Rossi¹, Mary-Anne Hartley¹, Patrik Castiglioni¹, Florence Prevel¹, Ricardo Martin¹, Chantal Desponds¹, Lon-Fye Lye², Stefan K. Drexler¹⁺, Walter Reith³, Stephen M. Beverley², Catherine Ronet¹, Nicolas Fasel^{1*}

¹Department of Biochemistry, University of Lausanne, 1066 Epalinges, Switzerland

²Department of Molecular Microbiology, Washington University, School of Medicine, St.Louis, MO 63110, USA.

³Department of Pathology and Immunology, University of Geneva, 1211 Geneva, Switzerland

*Correspondence: nicolas.fasel@unil.ch (N.F)

⁺Present Address: Biozentrum, University of Basel, Basel, Switzerland

Running title

Leishmania RNA virus promotes macrophage survival

Summary

Some strains of the protozoan parasite *Leishmania guyanensis* (L.g) harbor a viral endosymbiont called *Leishmania* RNA virus 1 (LRV1). LRV1 recognition by TLR-3 increases parasite burden and lesion swelling in vivo. However, the mechanisms by which anti-viral innate immune responses affect parasitic infection are largely unknown. Upon investigating the mammalian host's response to LRV1, we found that miR-155 was singularly and strongly upregulated in macrophages infected with LRV1+ L.g when compared to LRV1- L.g. LRV1-driven miR-155 expression was dependent on TLR-3/TRIF signaling. Furthermore, LRV1-induced TLR-3 activation promoted parasite persistence by enhancing macrophage survival through Akt activation in a manner partially dependent on miR-155. Pharmacological inhibition of Akt resulted in a decrease in LRV1-mediated macrophage survival and consequently decreased parasite persistence. Consistent with these data, miR-155-deficient mice showed a drastic decrease in LRV1-induced disease severity, and lesional macrophages from these mice displayed reduced levels of Akt phosphorylation.

Introduction

Macrophages are host cells for several obligate intracellular protozoan parasites such as *Leishmania spp.*, *Trypanosoma cruzi* and *Toxoplasma gondii* (Sacks and Sher, 2002). Upon infection, macrophages shape the early phases of immunity by sensing pathogen-associated molecular patterns (PAMPs) through pathogen recognition receptors (PRRs). The family of Toll-like receptors (TLRs) is one of the most intensively studied classes of PRRs. The engagement of TLRs to their cognate ligands leads to a cascade of events including the recruitment of various adaptor molecules such as myeloid differentiation primary response gene 88 (MyD88), MyD88 adaptor-like, TIR-domain containing adaptor-inducing IFN- β (TRIF), and the TRIF-related adaptor molecule. The MyD88 adaptor protein is involved in the signaling of all TLRs except the double-stranded RNA (dsRNA) receptor TLR-3, which exclusively recruits TRIF. Both MyD88-dependent and –independent TLR pathways transduce signals through conserved inflammatory signaling pathways, inducing Interleukin-6 (IL-6) and tumor necrosis factor- α (TNF- α) secretion. TLR stimulation also promotes the activation of phosphatidylinositol 3-kinase (PI3K)/Akt. In addition to these pathways, TRIF-dependent TLR signaling induces the phosphorylation of interferon response element 3 (IRF-3), leading to the transcription of IFN- β (Rakoff-Nahoum and Medzhitov, 2009).

TLR activation of innate cells is involved in the development of parasitocidal immunity by presenting parasitic antigens to T cells (Iwasaki and Medzhitov, 2004). Antigen-activated CD4⁺ T cells are a major source of IFN- γ , which is a key mediator of anti-*Leishmania* effector genes in macrophages (Bogdan et al., 2000). However, excessive TLR stimulation can be detrimental to the host in chronic infectious

diseases by leading to progressive tissue damage and fatal systemic disorders. For example, TLR-3 recognition of an endosymbiotic dsRNA virus within *Leishmania guyanensis* (L.g) increases the virulence of its microbial host and induces a hyper-inflammatory response by exploiting the innate recognition of its mammalian host (Ives et al., 2011).

In addition to initiating inflammation and adaptive immunity, TLRs are known to be involved in macrophage survival (Lombardo et al., 2007). Certain bacterial species hinder TLR-4 mediated cell survival factors to induce macrophage apoptosis, proposing a mechanism for bacterial immune evasion (Hsu et al., 2004; Park et al., 2005). Several viral species are reported to extend the host cell viability by inducing the PI3K/Akt signaling pathway to achieve latent and/or chronic infection (Cooray, 2004). Similarly, intracellular protozoan parasites can promote host cell survival by activating pro-survival signaling pathways or interrupting the host cell apoptotic machinery (Heussler et al., 2001). For example, infection of a murine macrophage cell line with *Leishmania spp.* induces PI3K/Akt signaling and grants them protection against apoptosis (Ruhland et al., 2007). Taken together, the subtle equilibrium between death and survival of innate cells has a determining impact on the outcome of microbial infections.

Akt, a member of the protein kinase B family, is a serine threonine kinase that regulates numerous substrates involved in cell survival, cellular growth and metabolism. For instance, TLR-3-induced endogenous phosphorylation of Akt in primary murine macrophages leads to the degradation of Forkhead box O3 (Foxo3a), a transcription factor that regulates genes involved in cell death (Litvak et al., 2012). Furthermore, Akt positively regulates the mammalian target of rapamycin 1 (mTOR1), which plays a key role in cell survival and growth by modulating mRNA

translation and many cellular processes in innate cells (Weichhart et al., 2015). The activating serine 2448 phosphorylation of mTOR1 by Akt leads to the phosphorylation of ribosomal protein S6 kinase (S6K), which promotes mRNA translation (Huang and Houghton, 2003).

Another important component of TLR stimulation is the expression of small non-coding RNAs, named microRNAs, which regulate genes at the post-transcriptional level, culminating in the degradation of the transcript or the inhibition of translation (Valencia-Sanchez et al., 2006). In macrophages, microRNA-155 (miR-155) is the only microRNA that is significantly up-regulated in response to polyinosinic:polycytidylic acid (poly I:C), a synthetic dsRNA ligand for TLR-3 (O'Connell et al., 2007). MiR-155 is also classified as an oncogenic microRNA. The overexpression of miR-155 in mice causes a myeloid proliferative disorder, which is at least partially due to Akt-mediated cell survival and proliferation (O'Connell et al., 2008), indicating the oncogenic potential of a TLR-induced microRNA.

In this study, we asked which microRNAs were modulated in macrophages in the presence of L.g endosymbiont LRV1 and investigated how and by which mechanism(s) LRV1 contributed to increased pathology.

Results

MiR-155 is the uniquely expressed microRNA due to LRV1/TLR-3/TRIF signaling

To determine the impact of LRV1 on the miRNA expression profile, murine bone-marrow macrophages (BMMs) were incubated with LRV1+ L.g or LRV1- L.g parasites for 10 hours followed by a miRNA microarray analysis performed on total

RNA. Out of 1179 miRNAs, miR-155 was the only miRNA significantly up-regulated by LRV1+ L.g infection in comparison to LRV- L.g (**Figure 1A**). To verify this result, isolated RNA from LRV1+ L.g or LRV1- L.g infected macrophages was reverse transcribed into complementary DNA (cDNA) using a stem-loop primer approach (Hurley et al., 2012). cDNAs were then used to quantify mature miR-155 by real-time PCR (RT-PCR). Consistent with the microRNA microarray data, miR-155 was drastically up-regulated in response to poly I:C treatment and LRV1+ L.g infection (**Figure 1B**). These findings demonstrated that the dsRNA endosymbiont within L.g altered the miRNAome profile of host macrophages and induced the expression of miR-155.

MiR-155 is located in third exon of the non-protein coding B cell integrated cluster (*BIC*) gene (Tam, 2001). To examine the kinetics of miR-155 induction in BMMs following various stimuli, the expression of both *BIC* mRNA and the mature form of miR-155 were monitored for 24 hours post-infection using RT-PCR. In the presence of LRV1 or poly I:C, miR-155 and *BIC* gene were detected after 2 hours, with a peak at 10 hours post-infection (**Figures 1C-D**). MiR-155 expression stabilized after 10 hours post-incubation, while the transcript level of *BIC* was strongly down-regulated in macrophages incubated with LRV1+ L.g and poly I:C after 24 hours (**Figures 1C-D**). Upon LRV1- L.g infection, *BIC* remained almost undetectable during the 24-hour time course (**Figures 1D**). In miR-155^{-/-} deficient mice, a β -galactosidase reporter gene replaces the third exon of *BIC* allowing the measurement of *BIC* promoter activity (Thai et al., 2007). LRV1+ L.g and LRV1- L.g infected miR-155^{-/-} BMMs were lysed and cell lysates were tested for β -galactosidase by immunoblotting (**Figure 1E**). We observed that the β -galactosidase level peaked after 10 hours incubation

with LRV1+ L.g or poly I:C. Comparatively, LRV1- L.g infection induced residual β -galactosidase expression (**Figure 1E**).

The LRV1 dsRNA genome is an agonist of TLR-3, which signals through TRIF adaptor protein (Ives et al., 2011). To investigate whether LRV promotes miR-155 expression through the TLR-3/TRIF signaling pathway, BMMs derived from WT, TLR3^{-/-}, and TRIF^{LPS2} were infected with LRV1+ L.g or LRV1- L.g. Poly I:C treatment was used as a positive control. Both LRV1 and poly I:C-induced miR-155 expression required functional TLR-3 and TRIF molecules since the ablation of either TLR-3 or TRIF abrogated miR-155 expression (**Figure 1F**). These data indicated that the TLR-3/TRIF signaling pathway initiated the expression of miR-155 upon sensing LRV1 or synthetic dsRNA.

LRV1 mediated miR-155 expression confers increased parasite burden and severity of pathology in mice

The role of miR-155 in the development of disease pathology was evaluated in vivo by infecting WT and miR-155^{-/-} mice in the footpad. A drastic decrease in footpad swelling and reduced parasite burden was observed in miR-155^{-/-} mice infected with LRV1+ L.g at the peak of infection (**Figures 2A-B**). In the case of LRV1- L.g infection, no significant difference in disease pathology was detected between WT and miR-155^{-/-} mice (**Figures 2A-B**). These findings suggested that LRV1 mediated host miR-155 expression played a crucial role in the survival of LRV1+ L.g parasites in mice.

Since miR-155 has also been shown to be required for the normal function of B cells and antibody secretion (Rodriguez et al., 2007; Thai et al., 2007), we decided to determine the impact of B cells on L.g infection. WT mice and mice lacking mature B

cells (Jh^{-/-}) were infected with LRV1+ L.g. Infected WT and B cell deficient mice displayed similar footpad swelling and parasitemia profiles (**Figures S1A and S1B**). We additionally examined B cell responses of miR-155 deficient mice infected with LRV1+ L.g by measuring total serum anti-LRV1 capsid immunoglobulin G (IgG) titers. Infected miR-155^{-/-} mice produced reduced titers of anti-LRV1 capsid IgG compared to infected WT mice (**Figure S1C**). These data suggested that B cells and the antibody response were not involved in the pathology of *Leishmania* infection, and were not essential for the LRV1+ L.g parasite resistant phenotype of miR-155^{-/-} mice.

It has also been reported that CD4⁺ T cells lacking miR-155 secrete more IL-4 but similar levels of IFN- γ compared to WT CD4⁺ T cells in in vitro differentiation conditions (Rodriguez et al., 2007). IFN- γ , which is predominantly secreted by CD4⁺ T cells, augments macrophage parasitocidal activity while IL-4 suppresses it (Sacks and Sher, 2002). Therefore, we evaluated the role of CD4⁺ T cells, which are required for controlling *Leishmania* parasites in our model of infection. To determine the impact of miR-155 on IL-4 and IFN- γ secreting CD4⁺ T cells during L.g infection, we used intracellular flow-cytometry analysis on the popliteal lymph node cells from WT and miR-155^{-/-} mice infected either with LRV1+ L.g or LRV1- L.g at the peak of infection. Our results showed that the number and percentages of IFN- γ and IL-4 secreting CD4⁺ T cells in LRV1+ L.g infected mice were similar compared to LRV1- L.g infected mice (**Figures 2C and S2**). These data indicated that the reduced disease progression in miR-155^{-/-} mice in response to LRV1+ L.g did not arise from an IFN- γ /IL-4 imbalance.

To further investigate the role of T cells in LRV1+ L.g infection, WT and miR-155^{-/-} mice were injected with anti-CD4 depleting antibody 5 days prior to infection and on

a weekly basis until 6 weeks post infection (**Figure S3A**). We verified the efficiency of the antibody-mediated depletion using flow-cytometry (**Figures S3B and S3C**). Interestingly, CD4 depletion caused a significant decrease in footpad swelling at 2-3 weeks post-infection both in LRV1+ L.g infected WT and miR-155^{-/-} mice (**Figure 2D**). We also observed that the resolution of footpad swelling was impaired in both LRV1+ L.g infected WT and miR-155^{-/-} mice after week 5 (**Figure 2D**). This data indicated that CD4⁺ cells contributed to lesion development early in LRV1+ L.g infection in a miR-155-independent manner and were required for the LRV1+ L.g infection resolution.

We analyzed parasite load in CD4-depleted WT and miR-155^{-/-} mice infected with LRV1+ L.g. We found that CD4-depletion had no effect on parasite burden in WT mice but led to a significant increase in parasite load in LRV1+ L.g infected miR-155^{-/-} mice at the peak of infection (**Figure 2E**). These data suggested that CD4⁺ T cells were required for control of LRV1+ L.g during the earlier phases of infection in miR-155^{-/-} mice but not in WT mice that probably have a compensatory source of IFN- γ other than CD4⁺ T cells in this time frame.

To better understand the possible impact of IFN- γ on the resistant phenotype of miR-155^{-/-} mice against LRV1+ L.g infection, we crossed miR-155^{-/-} mice with mice lacking IFN- γ to generate IFN- γ x miR-155 double-knockout (DKO) mice and infected these mice with LRV1+ L.g parasites. Our data showed that the lesion size of infected IFN- γ ^{-/-} and DKO mice were similar and were higher than their IFN- γ sufficient counterparts (**Figure 2F**). These findings showed that IFN- γ is essential for the clearance of L.g both in WT and miR-155^{-/-} mice.

Macrophages lacking miR-155 do not exhibit any changes in the LRV1-mediated hyper-inflammatory response

TLR-3 recognition of LRV1 induces a hyper-inflammatory response in macrophages, leading to the secretion of pro-inflammatory cytokines and an increase in infection severity in mice (Ives et al., 2011). We thus tested whether a deficiency in miR-155 expression could affect the LRV1-mediated pro-inflammatory cytokine profile in macrophages. BMMs were treated with poly I:C, or infected with LRV1+ L.g or LRV1- L.g. The supernatants were assayed for IL-6 and TNF- α . As shown previously, WT BMMs secreted IL-6 and TNF- α after 24 hours in the presence of poly I:C or LRV1+ L.g (**Figure 3A**). The TLR-3 activation of miR-155^{-/-} BMMs yielded similar cytokine profiles to WT macrophages, providing evidence that miR-155 did not play a role in the inflammatory response to LRV1.

We subsequently evaluated whether miR-155 deficiency had an impact on IRF3 activation, which in turn could lead to a decrease in the mRNA and protein level of IFN- β . WT BMMs along with macrophages deficient in miR-155 or TLR3 were infected with LRV1+ L.g, LRV1- L.g, or treated with poly I:C. We observed that in the presence of LRV1+ L.g or poly I:C, IRF-3 phosphorylation occurred as early as 2 hours following stimulation and became undetectable after 6 hours (**Figure 3B**). To compare the IRF3 phosphorylation levels between WT, TLR3^{-/-} and miR-155^{-/-} in response to infection, the cells were lysed 2 hours following infection. A change was not observed in IRF-3 phosphorylation in response to LRV1+ L.g infection or poly I:C between WT and miR-155^{-/-} BMMs (**Figure 3C**). As expected, the phosphorylated form of IRF-3 was undetectable under all conditions in TLR3^{-/-} infected macrophages (**Figure 3C**). Consistent with these findings, IFN- β was not significantly different between LRV1+ L.g infected WT and miR-155^{-/-} macrophages at either the

transcriptional or protein level (**Figures 3D and 3E**). These data ruled out the hypothesis that the absence of miR-155 could decrease the hyper-inflammatory responses arising from the innate sensing of LRV1.

LRV1+ L.g infection promotes activation of the PI3K/Akt signaling pathway

The infection of macrophages with *Leishmania* parasites activates the PI3K/Akt signaling pathway (Ruhland et al., 2007), which is regulated, in part, by miR-155 in TLR-stimulated macrophages (O'Connell et al., 2009). We thus asked whether the infection of macrophages with LRV1+ L.g or LRV1- L.g promoted activation of Akt via miR-155. We analyzed Akt and its targets by immunodetection in cell lysates of BMMs incubated with medium, poly I:C, LRV1+ L.g or LRV1- L.g. At 2 hours post-infection, the phosphorylation of Akt was increased in all conditions except in the medium-treated cells. Phosphorylated Akt levels in LRV1- L.g infected macrophages was reduced after 6 hours, but was still evident after 10 hours in LRV1+ L.g infection and poly I:C stimulation. Corresponding to these results, the level of pro-apoptotic Foxo3a gradually decreased in macrophages incubated with LRV1+ L.g or poly I:C, which is in accordance with a pro-survival effect of AKT (Litvak et al., 2012). We observed that the phosphorylation of GSK3- β was substantially greater in the presence of LRV1 or poly I:C at 6 hours post-infection when compared to LRV1- L.g infection (**Figure 4A**). We also detected an increase in mTOR and S6K phosphorylation in WT macrophages incubated with LRV1+ L.g, LRV1- L.g, or poly I:C for 2 hours (**Figure 4A**). Comparatively, we found higher levels of phosphorylated mTOR and S6K in macrophages incubated with LRV1+ L.g and poly I:C for 6 and 10 hours (**Figure 4A**). Of note, we showed that LRV1 or poly I:C-mediated Akt activation in macrophages could be abrogated upon pre-treatment with the Akt

inhibitor MK2206, or the PI3K inhibitor wortmanin (**Figure S4**). Thus, L.g infection of macrophages promoted activation of the Akt dependent pro-survival signaling pathway, which was intensified and prolonged in the presence of LRV1. Since LRV1+ L.g infection elicited an increase in Akt phosphorylation in macrophages 10 hours post infection, we investigated the role of miR-155 and TLR-3 in LRV1 mediated Akt activation. Protein levels of phosphorylated Akt and its targets were evaluated in WT, miR-155^{-/-} and TLR3^{-/-} macrophage lysates at 10 hours post-infection. It was observed that LRV1 mediated-Akt activation and Akt-dependent modulation of its targets relied on TLR-3, whilst miR-155 was partly involved in LRV1-mediated Akt activation (**Figures 4B and 4C**). Since miR-155 deficiency in TLR-stimulated macrophages results in an approximately 1.5 fold-increase in protein levels of the Src homology 2 domain-containing inositol-5-phosphatase 1 (SHIP1), a negative regulator of the PI3K/Akt signaling pathway (O'Connell et al., 2009), we investigated the changes in the SHIP1 protein level in WT, miR-155^{-/-} and TLR-3^{-/-} macrophages in response to LRV1 at 24 hours post-infection. As previously reported, we observed a 1.5 fold increase in the protein level of SHIP1 in LRV1+ L.g infected miR-155 deficient macrophages compared to their WT counterparts (**Figure S5A and S5B**), indicating that LRV1-mediated miR-155 expression could induce Akt activation by modulating SHIP1 protein levels. To determine whether miR-155 contributed to Akt activation in infected animals, we performed flow-cytometry analysis to measure phosphorylated Akt levels in lesional macrophages from LRV1+ L.g or LRV1- L.g infected WT and miR-155^{-/-} infected mice at 4 weeks post-infection (**Figure S6**). We found that lesional macrophages from infected miR-155^{-/-} mice displayed a significant reduction in phosphorylated Akt levels in comparison to WT infected mice (**Figure 4D**), whereas no significant

difference was observed in LRV- L.g infected WT or miR-155^{-/-} mice. Taken together, our results indicated that miR-155 was involved in the TLR-3 mediated activation of the pro-survival PI3K/Akt signaling pathway in macrophages infected with LRV1+ L.g.

TLR-3 mediated cell survival is dependent on TLR ligand concentration and Akt activation

Studies using knock-out animal models have shown that *Leishmania* molecules interact with several TLRs, however current knowledge on the identity and function of these molecules and their cognate TLRs is limited (Ives et al., 2014). Our results demonstrated that LRV1 drastically enhanced the L.g-mediated activation of the pro-survival signaling pathway Akt, suggesting that the innate recognition of L.g through other TLRs could induce the activation of Akt. Thus, we raised the question on how TLR-mediated Akt activation affected the cellular fitness of macrophages in terms of cell survival. To this end, we performed high content microscope analysis of WT and miR-155^{-/-} macrophages pretreated with DMSO or MK2206, an allosteric Akt inhibitor, and then incubated with various TLR and nucleotide-binding oligomerization domain-containing protein (NOD) ligands for 48 hours. We found that the ligation of certain TLRs did not induce cell survival such as TLR-1/2 and TLR-5 (**Figures 5A-B**). In contrast, TLR-2/6, TLR-4, and TLR-7 ligation promoted macrophage survival. This effect was however not diminished by MK2206 pre-treatment at higher concentrations of TLR ligand (**Figures 5A-B**). TLR-3 binding induced cell survival in a dose- and Akt-dependent manner, while Akt-dependent cell survival in the presence of TLR-2 and TLR-9 ligands was only observed at the highest agonist concentration. The fold change in WT macrophage numbers were

similar to miR-155 macrophage numbers in all conditions except for macrophages treated with the TLR-9 ligand ODN 2006 (**Figures 5A-B**). Taken together, these findings showed that the engagement of certain TLRs promoted macrophage survival in an Akt-dependent or –independent manner and this effect varied depending on the TLR-ligand concentration.

LRV1+ L.g induced macrophage survival through the TLR-3/Akt axis is partially dependent on miR-155

Our results demonstrated that TLR-3 stimulation promoted macrophage survival through the Akt signaling pathway. To determine whether LRV1 mediated-Akt activation promoted parasite persistence by inducing macrophage survival through miR-155 or TLR-3, BMMs were pre-incubated with DMSO or MK2206 and then infected with a multiplicity of infection (MOI) of 1 of L.g parasites either containing LRV1 or not. We found that the infection of WT and miR-155^{-/-} macrophages with 1 MOI of LRV1+ L.g increased macrophage survival. This effect was reversed by MK2206 pre-treatment in WT BMMs, but not in miR-155^{-/-} and TLR-3^{-/-} BMMs (**Figures 6A-B**). Confirming our previous work (Zangger et al., 2014), the presence of LRV1 within parasites did not affect the parasite number per macrophage but infected macrophage survival (**Figure 6C**). Taken together, these results indicated that LRV1 dsRNA genome ligation to TLR-3 promoted macrophage survival and therefore parasite persistence by activating the Akt signaling pathway in a miR-155 partially dependent manner.

Discussion

Our results demonstrated that LRV1 was able to exploit the TLR-3/miR-155/Akt signaling axis to enhance macrophage survival and persistence of intracellular

Leishmania parasites. Interestingly, the miR-155/Akt signaling pathway is known to cause myeloid proliferative disorder in both human and mice (O'Connell et al., 2008; Xue et al., 2014). However, a deficiency in the myeloid compartment is not observed in miR-155^{-/-} mice under basal conditions (Rodriguez et al., 2007), suggesting that miR-155 function requires induction. It is known that miR-155 is the only microRNA up-regulated upon TLR-3 ligation in macrophages and that other TLR receptor agonists also promote miR-155 expression (O'Connell et al., 2007). Concurrently, we found that miR-155 was the only microRNA among 1179 miRNAs, which was significantly up-regulated in the presence of LRV1 in a TLR-3/TRIF dependent manner. We observed that LRV1- L.g infection only weakly induced miR-155 and *B/C* expression, suggesting that the innate recognition of parasites promoted only a slight increase in miR-155 expression through PRRs other than TLR-3. We found that mice deficient in miR-155 had significantly reduced disease pathology when infected with LRV1+ L.g, but not with LRV1- L.g. These results indicated that LRV1 used host miR-155 as a persistence mechanism, a situation evocative of certain Herpesviruses which exert their virulence via the pathogenic overexpression of miR-155 from either viral- or host-origin (Gottwein et al., 2007; Linnstaedt et al., 2010; Zhao et al., 2011). In this regard, whether other protozoan parasites containing viruses belonging to the *Totiviridae* family can subvert the host immune system through TLR-3/miR-155 remains to be determined.

MiR-155 deficiency in mice was shown to be protective against T- and B-cell driven autoimmune disorders such as rheumatoid arthritis (Blumel et al., 2011; Kurowska-Stolarska et al., 2011), experimental autoimmune encephalomyelitis (O'Connell et al., 2010), and systemic lupus erythematosus (Thai et al., 2013). However, interestingly, in serum or autoantibody transfer arthritis models, which are

predominantly driven by innate cells, the severity of joint inflammation is not different between WT and miR-155^{-/-} mice (Bluml et al., 2011; Kurowska-Stolarska et al., 2011). In addition, WT and miR-155^{-/-} macrophages secrete similar levels of TNF- α after in vitro stimulation with autoantibody immune complexes (Kurowska-Stolarska et al., 2011). Other studies show that the impact of miR-155 on the pro-inflammatory cytokine profile of LPS-stimulated macrophages (Androulidaki et al., 2009) and other cell types (Tili et al., 2007) at the protein level by transfecting a microRNA mimic or antagonist. However, we did not observe a difference in the pro-inflammatory cytokine profile between WT and miR-155^{-/-} primary murine macrophages in response to poly I:C or LRV1+ L.g infection in terms of the secretion of pro-inflammatory cytokines (TNF- α , IL-6 and IFN- β), the expression of IFN- β mRNA, and the phosphorylation of IRF-3. These results might be explained by the difference in stimuli, but it should be noted that transfecting microRNA mimics or antagonists could cause an increase in the expression of endogenous microRNA targets due to the overexpression-mediated saturation of the intracellular protein complex which guides microRNAs to its target mRNA (Khan et al., 2009).

We found that IFN- γ and IL-4 secreting CD4⁺ T cell numbers of LRV1+ L.g infected WT mice were not different from LRV1+ L.g infected miR-155^{-/-} mice at the peak of infection, although, it was previously shown that CD4⁺ T cells of miR-155 deficient mice secrete more IL-4 and similar levels IFN- γ under in vitro differentiation conditions (Rodriguez et al., 2007). However, the IFN- γ and/or IL-4 secretion of ex vivo WT and miR-155 CD4⁺ T cells were found to be similar in different biological settings (Kurowska-Stolarska et al., 2011; O'Connell et al., 2010), suggesting that miR-155 affects CD4⁺ T cell plasticity in a condition-specific manner. Interestingly, we showed that CD4⁺ cells mediated footpad swelling in mice infected with LRV1+

L.g through miR-155-independent mechanisms. Thus, further studies are required to understand the role of CD4⁺ T cell lineages in this miR155-independent LRV1-mediated disease pathology.

We demonstrated that miR-155^{-/-} mice, unlike WT mice, required CD4⁺ T cells to control parasite growth early on infection. Further, it is known that miR-155 deficiency impairs the effector function of other-IFN- γ -producing cells, such as NK cells (Trotta et al., 2012), which can play a compensatory role in the restriction of parasite growth in the absence of CD4⁺ T cells in the early phases of infection (Scharton and Scott, 1993). In our study, we found that both WT and miR-155^{-/-} mice were not able to control LRV1+ L.g infection in the absence of IFN- γ mediated immune pressure, suggesting that IFN-g is absolutely essential to control infection either in WT or in miR-155^{-/-} mice.

Several reports have proposed that the infection of macrophages with *Leishmania spp.* promotes parasite persistence by enhancing macrophage survival (Akarid et al., 2004; Moore and Matlashewski, 1994; Moore et al., 1994; Ruhland et al., 2007).

Addressing the question on how the innate recognition of LRV1 modify host cells to induce the survival of its microbial host, we found that LRV1 induced the phosphorylation of the pro-survival protein kinase Akt through TLR-3 in a miR-155 partially dependent manner. Consistent with a previous study, our findings supported that miR-155 could modulate the PI3K/Akt signaling pathway by regulating SHIP1 protein expression (O'Connell et al., 2009). Functionally, our data showed that neither the LRV status of L.g nor deficiency of TLR-3 and miR-155 in macrophages had an impact on the number of parasites per macrophage in vitro. We cannot, however, exclude the involvement of TLR-3 expressing phagocytic cells, other than macrophages, which can act as host cells for *Leishmania* parasites, in the miR-155

deficiency mediated protection against LRV1+ L.g infection in mice. Nonetheless, our findings revealed a virulence mechanism in LRV1+ L.g infection, whereby LRV1 conferred a survival advantage to its parasite host by promoting the survival of infected macrophages, which are the definitive host cells for *Leishmania*, through a TLR3/miR-155/Akt signaling circuit. These results highlighted the potential clinical importance of oncogenic kinases during leishmaniasis, and identified several potential therapeutic targets to treat and prevent the disfiguring complications of cutaneous leishmaniasis.

Experimental Procedures

Animals

All animal protocols described in this report were approved by the Swiss Federal Veterinary Office (SFVO), under the authorization numbers 2113.1 and 2113.2.

Animal handling and experimental procedures were undertaken with strict adherence to ethical guidelines set out by the SFVO and under inspection by the Department of Security and Environment of the State of Vaud, Switzerland. Details are given in the Supplemental Experimental Procedures.

Parasite Culture

Parasites were cultured at 26°C in complete Schneider's medium with L-glutamine (Sigma-Aldrich®), supplemented with 1% penicillin/streptomycin (Amimed®) and 20% Fetal Calf Serum (FCS) (PAA®). The parasites were passaged in culture for not more than 5 passages, and isolated from mouse footpads to maintain their virulence. Details are given in the Supplemental Experimental Procedures.

Macrophage infection

The femurs and tibias of naïve mice were washed with medium containing 1% P/S to extract cells, which were differentiated into bone marrow derived macrophages

(BMMs) for 6 days using complete DMEM supplemented with L-929 (EACC cell line, Sigma-Aldrich®) conditioned media at 37°C. BMMs were seeded on culture plates, and incubated overnight. BMMs were infected with stationary phase LRV1+ or LRV1- L.g at MOI of 10 parasite per macrophage, unless otherwise indicated. BMMs were also treated with poly I:C (Invivogen®) at 2µg/ml or pretreated with DMSO (Sigma-Aldrich®) or 5µM MK2206 (Apexbio) for 1 hour.

MicroRNA microarray

Four independent experiments were performed. In each experiment, macrophages derived from 2 individual C57BL/6 mice were either infected with LRV1+ ,or LRV1- L.g ,or lysed with RNAzol®RT (Mrcgene) after 10 hours post infection. As a control, macrophages were treated with medium or poly I:C for post-array verification by RT-PCR. Total RNA was isolated from samples and microRNA microarray (Agilent mouse miRbase v18.0) was performed following the manufacturer's instruction. Details are given in the Supplemental Experimental Procedures.

The quantification of microRNA and mRNA using quantitative real time-PCR

The miR-16 and miR-155 levels were quantified with stem-loop RT-PCR. The abundance of mRNA and pre-miRNA were quantified with RT-PCR using Taqman® probe or SYBR Green (Roche®)-based detection. The results were normalized against 60S ribosomal protein L32 (L32) for mRNA and miR-16 for microRNA. Details are given in the Supplemental Experimental Procedures.

Mice infection and the quantification of parasite burden by bioluminescence

Age-matched mice were infected with 1×10^6 stationary *Leishmania* parasites in both hind footpads of mice. Change in footpad thickness was monitored on a weekly basis. As described previously (Ives et al., 2011), parasite burden were quantified in mice by intra-peritoneally injecting D-Luciferin sodium salt (Regis Technologies®) in

1xPBS at a concentration of 150mg/kg. The images were acquired and analyzed using a Xenogen Lumina II imaging system (IVIS®); Living Image® software. Mice were anesthetized with isofluorane during the image acquisition. Oval region of interest (ROI) were set on footpads and the tail to determine the parasite burden or the background, respectively. Bioluminescent signals were expressed in units of photons per second (P/s).

Flow cytometry analysis

Popliteal lymph nodes (PLNs) or footpad lesions (FLs) were harvested from infected mice at the peak of infection. A single cell suspension was prepared from FLs and PLNs with or without collagenase /DNaseI treatment, respectively. Cells isolated from PLNs were counted before PMA/ionomycin in vitro stimulation. Extracellular staining was performed using anti-mouse CD4 and CD8 antibodies. Cells were intracellularly stained for IFN- γ and IL-4 cytokines using an intracellular fixation and permeabilization buffer set, following manufacturer`s instructions (eBioscience®). Cells isolated from FLs were fixed and permeabilized as described before (Krutzik and Nolan, 2003), followed by staining with CD45, CD11b, CD11c, F4/80 and p-Akt (T308) antibodies. Samples were acquired in BD FACSVerser™ or LSR II flow cytometry, and analyzed using FlowJo software. Details are given in the Supplemental Experimental Procedures.

In vivo depletion of CD4 cells

Anti-CD4 GK1.5 monoclonal antibody was purified from hybridoma (GK1.5; ATCC) culture supernatant using affinity chromatography on HiTrap Protein-G columns (Amersham-Pharmacia, Freiburg, Germany). Mice were intraperitoneally injected with 500 μ g anti-CD4 GK1.5 antibody 5 days prior to infection and on a weekly basis

until 7 weeks post- infection. The splenocytes of mice were harvested to verify the efficiency of antibody-mediated depletion using flow cytometry.

The quantification of cytokine concentration in in vitro culture

The concentrations of TNF- α (eBioscience®), IL-6 (eBioscience®), and IFN- β (PBL, Interferon Source) in collected supernatants from treated macrophages were determined using enzyme-linked immuno-sorbent assay (ELISA) following manufacturer's instructions. The plates (Nunc-Immuno™) were read on a Synergy™ HT Multi-Mode Plate Reader (Biotek Instruments, Switzerland). Wavelength correction and background signals were subtracted from the absorbance values.

Western blot analysis

Cells were lysed using cell lysis buffer containing protease/phosphatase inhibitors. Cell lysates were run on SDS-PAGE, transferred to nitrocellulose membrane, and analyzed by Western blotting using antibodies specific for the indicated antigens. Details are given in the Supplemental Experimental Procedures.

High Content Microscopy

BMMs were counted with Vi-Cell® (Beckman Coulter) then seeded on 96 well tissue-culture treated clear bottom plates (Falcon®). After overnight incubation, cells were treated with DMSO (Sigma-Aldrich), or 5 μ M MK2206 (ApeXBio) for 1 hour.

Subsequent to a washing step, BMMs were treated with ligands in Multi-TLR array (Invivogen®) medium, poly I:C (2 μ g/ml), LRV1+ L.g or LRV1- L.g for 48 hours. Cells were fixed with freshly made %3.7 PFA in 1x PBS pH 7.4, stained with DAPI (Molecular Probes®) and Alexa488-Phalloidin (Molecular Probes®) then washed with 1xPBS using a Biotek® MultioFlo FX plate washer. 49 (7x7 square, total area 0.12mm²). Images were acquired from each well using ImageXpress Micro XLS, and

cell and parasite numbers were counted using an automated software program (MetaExpress®).

Accession Number

The ArrayExpress accession number for the microRNA microarray is E-MTAB-4413.

Statistical Analysis

All graphs were generated in GraphPad Prism. Unpaired Student's t-test and repeated measure two-way ANOVA tests were performed using Microsoft Excel and GraphPad Prism, respectively. We considered $P < 0.05$ and $P < 0.001$ for unpaired Student's t-test and repeated measure two-way ANOVA test with Bonferroni's post-test to be statistically significant, respectively. NS stands for a non-significant statistical difference. P values are shown as * for $P < 0.05$, ** for $P < 0.01$ and *** for $P < 0.001$.

Author Contributions

Conceptualization, R.O.E. and N.F.; Methodology, R.O.E. and N.F.; Investigation, M.Re., M.Ro., M.A.H., P.C., F.P., R.M., C.H., S.K.D., C.R., R.O.E., and N.F.; Resources L.F.L., W.R., and S.M.B. ;Writing- Original Draft R.O.E. and N.F.; Writing- Review & Editing W.R., S.M.B., C.R., R.O.E., and N.F.; Funding Acquisition M.A.H., C.R., S.M.B., and N.F.

Acknowledgments

We thank S. Hickerson and K. Owens for assistance with generation/handling of luciferase-expressing L.g. We thank K. Harshman and F. C. Barras (Center of Integrative Genomics, UNIL) for the microRNA microarray experiment. We thank D. Monreau and C.U. Eren for the assistance with the high content microscopy and S. Masina for critical reading of the manuscript. We thank the NCCR Geneva Access platform for providing the equipment for the high-content microscope experiments.

This work is funded by grants from the Swiss National fund for research (FNRS 310030-153204 and IZRJZ3_164176) (N.F.), the Institute for Arthritis Research (iAR), the COST action CM1307 SEFRI: C14.0070 (N.F.), the Pierre Mercier Foundation (M.A.H. and C.R.) and the NIH R56AI099364 -R01AI029646 (S.M.B.).

References

- Akarid, K., Arnoult, D., Micic-Polianski, J., Sif, J., Estaquier, J., and Ameisen, J.C. (2004). Leishmania major-mediated prevention of programmed cell death induction in infected macrophages is associated with the repression of mitochondrial release of cytochrome c. *Journal of leukocyte biology* 76, 95-103.
- Androulidaki, A., Iliopoulos, D., Arranz, A., Doxaki, C., Schworer, S., Zacharioudaki, V., Margioris, A.N., Tschlis, P.N., and Tsatsanis, C. (2009). The kinase Akt1 controls macrophage response to lipopolysaccharide by regulating microRNAs. *Immunity* 31, 220-231.
- Bluml, S., Bonelli, M., Niederreiter, B., Puchner, A., Mayr, G., Hayer, S., Koenders, M.I., van den Berg, W.B., Smolen, J., and Redlich, K. (2011). Essential role of microRNA-155 in the pathogenesis of autoimmune arthritis in mice. *Arthritis and rheumatism* 63, 1281-1288.
- Bogdan, C., Rollingshoff, M., and Diefenbach, A. (2000). Reactive oxygen and reactive nitrogen intermediates in innate and specific immunity. *Current opinion in immunology* 12, 64-76.
- Cooray, S. (2004). The pivotal role of phosphatidylinositol 3-kinase-Akt signal transduction in virus survival. *The Journal of general virology* 85, 1065-1076.
- Gottwein, E., Mukherjee, N., Sachse, C., Frenzel, C., Majoros, W.H., Chi, J.T., Braich, R., Manoharan, M., Soutschek, J., Ohler, U., and Cullen, B.R. (2007). A viral microRNA functions as an orthologue of cellular miR-155. *Nature* 450, 1096-1099.
- Heussler, V.T., Kuenzi, P., and Rottenberg, S. (2001). Inhibition of apoptosis by intracellular protozoan parasites. *International journal for parasitology* 31, 1166-1176.

Hsu, L.C., Park, J.M., Zhang, K., Luo, J.L., Maeda, S., Kaufman, R.J., Eckmann, L., Guiney, D.G., and Karin, M. (2004). The protein kinase PKR is required for macrophage apoptosis after activation of Toll-like receptor 4. *Nature* 428, 341-345.

Huang, S., and Houghton, P.J. (2003). Targeting mTOR signaling for cancer therapy. *Current opinion in pharmacology* 3, 371-377.

Hurley, J., Roberts, D., Bond, A., Keys, D., and Chen, C. (2012). Stem-loop RT-qPCR for microRNA expression profiling. *Methods in molecular biology* 822, 33-52.

Ives, A., Masina, S., Castiglioni, P., Prevel, F., Revaz-Breton, M., Hartley, M.A., Launois, P., Fasel, N., and Ronet, C. (2014). MyD88 and TLR9 dependent immune responses mediate resistance to *Leishmania guyanensis* infections, irrespective of *Leishmania* RNA virus burden. *PloS one* 9, e96766.

Ives, A., Ronet, C., Prevel, F., Ruzzante, G., Fuertes-Marraco, S., Schutz, F., Zangger, H., Revaz-Breton, M., Lye, L.F., Hickerson, S.M., *et al.* (2011). *Leishmania* RNA virus controls the severity of mucocutaneous leishmaniasis. *Science* 331, 775-778.

Iwasaki, A., and Medzhitov, R. (2004). Toll-like receptor control of the adaptive immune responses. *Nature immunology* 5, 987-995.

Khan, A.A., Betel, D., Miller, M.L., Sander, C., Leslie, C.S., and Marks, D.S. (2009). Transfection of small RNAs globally perturbs gene regulation by endogenous microRNAs. *Nature biotechnology* 27, 549-555.

Krutzik, P.O., and Nolan, G.P. (2003). Intracellular phospho-protein staining techniques for flow cytometry: monitoring single cell signaling events. *Cytometry. Part A : the journal of the International Society for Analytical Cytology* 55, 61-70.

Kurowska-Stolarska, M., Alivernini, S., Ballantine, L.E., Asquith, D.L., Millar, N.L., Gilchrist, D.S., Reilly, J., Ierna, M., Fraser, A.R., Stolarski, B., *et al.* (2011).

MicroRNA-155 as a proinflammatory regulator in clinical and experimental arthritis. *Proceedings of the National Academy of Sciences of the United States of America* *108*, 11193-11198.

Linnstaedt, S.D., Gottwein, E., Skalsky, R.L., Luftig, M.A., and Cullen, B.R. (2010). Virally induced cellular microRNA miR-155 plays a key role in B-cell immortalization by Epstein-Barr virus. *Journal of virology* *84*, 11670-11678.

Litvak, V., Ratushny, A.V., Lampano, A.E., Schmitz, F., Huang, A.C., Raman, A., Rust, A.G., Bergthaler, A., Aitchison, J.D., and Aderem, A. (2012). A FOXO3-IRF7 gene regulatory circuit limits inflammatory sequelae of antiviral responses. *Nature* *490*, 421-425.

Lombardo, E., Alvarez-Barrientos, A., Maroto, B., Bosca, L., and Knaus, U.G. (2007). TLR4-mediated survival of macrophages is MyD88 dependent and requires TNF- α autocrine signalling. *Journal of immunology* *178*, 3731-3739.

Moore, K.J., and Matlashewski, G. (1994). Intracellular infection by *Leishmania donovani* inhibits macrophage apoptosis. *Journal of immunology* *152*, 2930-2937.

Moore, K.J., Turco, S.J., and Matlashewski, G. (1994). *Leishmania donovani* infection enhances macrophage viability in the absence of exogenous growth factor. *Journal of leukocyte biology* *55*, 91-98.

O'Connell, R.M., Chaudhuri, A.A., Rao, D.S., and Baltimore, D. (2009). Inositol phosphatase SHIP1 is a primary target of miR-155. *Proceedings of the National Academy of Sciences of the United States of America* *106*, 7113-7118.

O'Connell, R.M., Kahn, D., Gibson, W.S., Round, J.L., Scholz, R.L., Chaudhuri, A.A., Kahn, M.E., Rao, D.S., and Baltimore, D. (2010). MicroRNA-155 promotes autoimmune inflammation by enhancing inflammatory T cell development. *Immunity* *33*, 607-619.

O'Connell, R.M., Rao, D.S., Chaudhuri, A.A., Boldin, M.P., Taganov, K.D., Nicoll, J., Paquette, R.L., and Baltimore, D. (2008). Sustained expression of microRNA-155 in hematopoietic stem cells causes a myeloproliferative disorder. *The Journal of experimental medicine* 205, 585-594.

O'Connell, R.M., Taganov, K.D., Boldin, M.P., Cheng, G., and Baltimore, D. (2007). MicroRNA-155 is induced during the macrophage inflammatory response. *Proceedings of the National Academy of Sciences of the United States of America* 104, 1604-1609.

Park, J.M., Greten, F.R., Wong, A., Westrick, R.J., Arthur, J.S., Otsu, K., Hoffmann, A., Montminy, M., and Karin, M. (2005). Signaling pathways and genes that inhibit pathogen-induced macrophage apoptosis--CREB and NF-kappaB as key regulators. *Immunity* 23, 319-329.

Rakoff-Nahoum, S., and Medzhitov, R. (2009). Toll-like receptors and cancer. *Nature reviews. Cancer* 9, 57-63.

Rodriguez, A., Vigorito, E., Clare, S., Warren, M.V., Couttet, P., Soond, D.R., van Dongen, S., Grocock, R.J., Das, P.P., Miska, E.A., *et al.* (2007). Requirement of bic/microRNA-155 for normal immune function. *Science* 316, 608-611.

Ruhland, A., Leal, N., and Kima, P.E. (2007). Leishmania promastigotes activate PI3K/Akt signalling to confer host cell resistance to apoptosis. *Cell Microbiol* 9, 84-96.

Sacks, D., and Sher, A. (2002). Evasion of innate immunity by parasitic protozoa. *Nature immunology* 3, 1041-1047.

Scharton, T.M., and Scott, P. (1993). Natural killer cells are a source of interferon gamma that drives differentiation of CD4+ T cell subsets and induces early

resistance to *Leishmania major* in mice. *The Journal of experimental medicine* *178*, 567-577.

Tam, W. (2001). Identification and characterization of human BIC, a gene on chromosome 21 that encodes a noncoding RNA. *Gene* *274*, 157-167.

Thai, T.H., Calado, D.P., Casola, S., Ansel, K.M., Xiao, C., Xue, Y., Murphy, A., Friendewey, D., Valenzuela, D., Kutok, J.L., *et al.* (2007). Regulation of the germinal center response by microRNA-155. *Science* *316*, 604-608.

Thai, T.H., Patterson, H.C., Pham, D.H., Kis-Toth, K., Kaminski, D.A., and Tsokos, G.C. (2013). Deletion of microRNA-155 reduces autoantibody responses and alleviates lupus-like disease in the Fas(*lpr*) mouse. *Proceedings of the National Academy of Sciences of the United States of America* *110*, 20194-20199.

Tili, E., Michaille, J.J., Cimino, A., Costinean, S., Dumitru, C.D., Adair, B., Fabbri, M., Alder, H., Liu, C.G., Calin, G.A., and Croce, C.M. (2007). Modulation of miR-155 and miR-125b levels following lipopolysaccharide/TNF-alpha stimulation and their possible roles in regulating the response to endotoxin shock. *Journal of immunology* *179*, 5082-5089.

Trotta, R., Chen, L., Ciarlariello, D., Josyula, S., Mao, C., Costinean, S., Yu, L., Butchar, J.P., Tridandapani, S., Croce, C.M., and Caligiuri, M.A. (2012). miR-155 regulates IFN-gamma production in natural killer cells. *Blood* *119*, 3478-3485.

Valencia-Sanchez, M.A., Liu, J., Hannon, G.J., and Parker, R. (2006). Control of translation and mRNA degradation by miRNAs and siRNAs. *Genes & development* *20*, 515-524.

Weichhart, T., Hengstschlager, M., and Linke, M. (2015). Regulation of innate immune cell function by mTOR. *Nature reviews. Immunology* *15*, 599-614.

Xue, H., Hua, L.M., Guo, M., and Luo, J.M. (2014). SHIP1 is targeted by miR-155 in acute myeloid leukemia. *Oncology reports* 32, 2253-2259.

Zangger, H., Hailu, A., Desponds, C., Lye, L.F., Akopyants, N.S., Dobson, D.E., Ronet, C., Ghalib, H., Beverley, S.M., and Fasel, N. (2014). *Leishmania aethiopica* field isolates bearing an endosymbiotic dsRNA virus induce pro-inflammatory cytokine response. *PLoS neglected tropical diseases* 8, e2836.

Zhao, Y., Xu, H., Yao, Y., Smith, L.P., Kgosana, L., Green, J., Petherbridge, L., Baigent, S.J., and Nair, V. (2011). Critical role of the virus-encoded microRNA-155 ortholog in the induction of Marek's disease lymphomas. *PLoS pathogens* 7, e1001305.

Figure Legends

Figure 1. LRV1 induced miR-155 expression through TLR-3/TRIF signaling

(A) MicroRNA microarray analysis was performed on total RNA extracted from WT BMMs infected with LRV1+ L.g and LRV1- L.g for 10 hours. Scatter plot shows \log_{10} -transformed normalized averaged intensity values (n=4) for each miRNA probe.

(B) A portion of WT BMMs generated in (A) were treated with medium or poly I:C (2 μ g/ml). RT-PCR was used to measure the abundance of the miR-155 in extracted RNA. The numbers represent relative miR-155 expression as fold induction over the medium treated condition subsequent to normalization with miR-16.

(C and D) Kinetic quantification of miR-16-normalized miR-155 (C) and L32-normalized *B/C* (D) expression in WT BMMs incubated with medium, poly I:C (2 μ g/ml), LRV1+ L.g or LRV1- L.g using RT-PCR.

(E) β -galactosidase western blot analysis of miR-155^{-/-} BMMs infected with LRV1+ L.g (+) or LRV1- L.g (-) at indicated time points. Cells treated with medium (as negative control) or with poly I:C (2 μ g/ml) (as positive control) were also blotted for β -galactosidase.

(F) The relative miR-155 expression levels of WT, TLR-3^{-/-} and TRIF Δ ^{LPS2} macrophages incubated with medium, poly I:C (2 μ g/ml), LRV1+ L.g or LRV1- L.g. Data are presented as mean \pm SEM from the pool of three independent experiments (C, D and F). Representative western blots were shown from three independent experiments (E). P values shown were calculated unpaired Student's t-test. ** P<0.01 and *** P<0.001.

Figure 2. MiR-155^{-/-} mice infected with LRV1+ L.g parasites had decreased disease pathology when compared to WT mice

(A and B) Hind footpads of WT and miR-155^{-/-} mice were infected with 1x10⁶ LRV1+ L.g or LRV1- L.g.

(A) The graph displays the weekly measurement of footpad swelling.

(B) Parasite burden was determined at 3 weeks after infection by bioluminescence imaging.

(C) Popliteal lymph nodes were collected from WT and miR-155 mice infected with LRV1+ L.g or LRV1- L.g on the footpad after 3 weeks infection. Intracellular FACS analysis was performed using primary ex vivo lymphocytes extracted stimulated with PMA/ionomycin to measure IL-4 and IFN- γ levels in CD4⁺ T cells (see also Figures S2).

(D-E) Mice were intraperitoneally injected with CD4-depleting antibody 5 days prior to LRV1+ L.g infection and then on weekly basis for 6 weeks. A group of mice were treated with PBS as a negative control (see also Figures S3 and S4).

(D) Footpad swelling of LRV1+ L.g infected WT and miR-155^{-/-} mice.

(E) Parasite load was measured by bioluminescence 4 weeks post-infection.

(F) The measurement of footpad swelling in WT, miR-155^{-/-}, IFN- γ and IFN- γ xmiR-155 DKO mice following of LRV1+ L.g infection.

Data shows mean \pm SD from representative experiments (n= 4-5 mice) of two (C-E) or three (A, B, F) independent experiments. Each dot in the scatter blot represents a footpad (B and E). Statistical significance is calculated using two-way ANOVA analysis with Bonferonni's posttest (A and D) and unpaired Student's t-test (B and E). Not significant (ns), * P<0.05, and *** P<0.001. See also Figure S1.

Figure 3. MiR-155^{-/-} macrophages exhibited similar proinflammatory cytokine response compared to WT macrophages in response LRV1+ L.g or poly I:C

(A-E) BMMs were infected with LRV1+ L.g (+) or LRV1- L.g (-). Cells were treated with medium or poly I:C (2 µg/ml) as a control for indicated times.

(A) The cell-free culture supernatant was collected 24 hours post-treatment from treated macrophages derived from WT, TLR-3^{-/-} and miR-155^{-/-} mice were assayed for IL-6 and TNF-α using ELISA.

(B) Total cell lysate of treated WT macrophages was analyzed by Western blot with IRF3-P, IRF-3, and γ-tubulin after 2, 6, and 10 hours infection.

(C) WT, TLR-3^{-/-} and miR-155^{-/-} BMMs were lysed after 2 hours and immunoblotted for the indicated antibodies.

(D) IFN-β mRNA levels were assayed after 2 hours incubation using RT-PCR. Values were normalized using L32. Transcript levels were calculated relative to unstimulated WT macrophages.

(E) Protein level of IFN-β was quantified in collected cell culture medium after 6 hours treatment.

Data are mean ± SD from three pooled independent experiments. Representative blots were showed from three independent experiments.

Figure 4. MiR-155 partially contributed TLR-3 dependent-Akt activation

(A-B) Macrophages incubated with medium, poly I:C, LRV1+ L.g (+), or LRV1- L.g (-) for indicated time(s). Cells were lysed and total protein lysates were immunoblotted for Foxo3a, GSK3-β, phosho-GSK3-β (Ser9), Akt, phosho-Akt (T308), S6K, phosho-S6K (Thr389), mTOR, phosho-mTOR (Ser2448) and γ-tubulin.

(A) Whole-cell lysate of WT macrophages after 2, 6, and 10 hours post-treatment were immunoblotted for the indicated proteins.

(B) Macrophages derived from WT, TLR-3^{-/-} and miR-155^{-/-} mice were incubated with indicated conditions for 10 hours, and whole cell lysates of indicated samples were subjected to western blot analysis with the indicated antibodies.

(C) Cell lysates described in (B) were immunoblotted for Akt, phospho-Akt (T308) and γ -tubulin. The levels of Akt (Thr308) phosphorylation were quantified by densitometric analysis. The data were normalized with total Akt and shown as fold increase of normalized Akt phosphorylation over Akt (T308) / Akt from medium-treated macrophages.

(D) Flow-cytometry analysis of the mean fluorescence intensity (MFI) of phosphorylated Akt (T308) in CD45⁺ CD11b⁺ CD11c⁻ F4/80⁺ lesional macrophages from LRV1+ L.g or LRV1- L.g infected WT and miR-155^{-/-} mice at 4 weeks post-infection. See also Figure S6.

Representative blots (A-B) and quantification (C) from at least three independent experiments are shown. The graph (D) shows pooled data from two independent experiments (n=2-5 mice). Data is expressed as mean \pm SD. Unpaired Student's t-test was used to measure statistical significance. Not significant (ns) and * P<0.05. See also Figure S3 and S4.

Figure 5. TLR-3 induced macrophage survival in an Akt-dependent manner

(A-B) WT (A) and miR-155^{-/-} (B) macrophages were seeded in 96-well plate and were pre-cultured with DMSO or MK2206 for 1 hour. Cells were treated with series of three ten-fold dilutions of TLR ligands, and were fixed after 48 hours. Macrophages were stained with DAPI (nucleus) and phalloidin (cytoskeleton), and were analyzed with high-content microscope. Images are in phalloidin channel and display an entire 96 well plate. Each square (352 μ Mx352 μ M) represents a well composing of 49 (7x7)

pictures taken by x40 lens. The fold increase in cell number were calculated by normalizing sample cell counts to the cell numbers within DMSO-treated well. Data represent mean \pm SD from two independent experiments with three biological replicates. See also Table S1.

Figure 6. LRV1 exploited TLR-3/miR-155/Akt pathway to promote the persistence of its microbial host

(A-C) WT, TLR-3^{-/-} and miR-155^{-/-} macrophages were infected with promastigotes of LRV1+ or LRV1- L.g at 1 MOI for 48 hours. Cells were fixed and processed for high-content analysis by staining with DAPI and phalloidin.

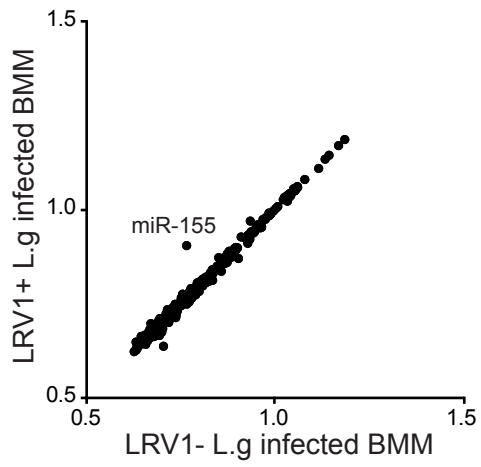
(A) A representative composite image of a well containing 7x7 pictures with 352 μ Mx352 μ M images from each condition were displayed in phalloidin channel.

(B) Relative macrophage number was quantified by normalizing cell numbers of the samples to the cell count of the medium-treated WT macrophages.

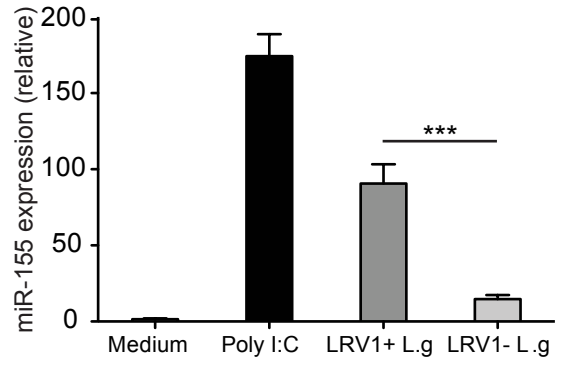
(C) Parasite load in macrophages described in (B) were quantified.

Mean \pm SD were calculated from two independent experiments with three biological replicates in triplicate. Data were analyzed unpaired Student's t-test. Not significant (ns), * P<0.05, ** P<0.01 and *** P<0.001.

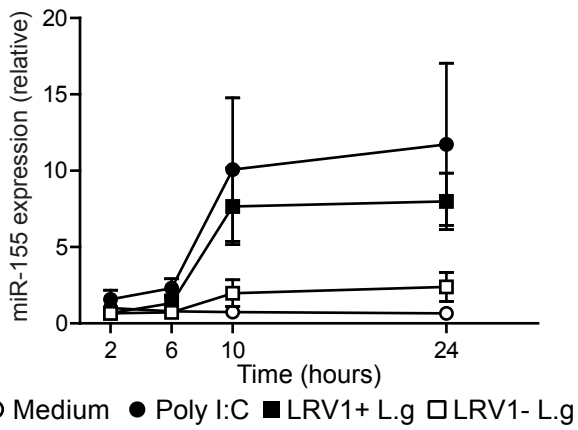
A



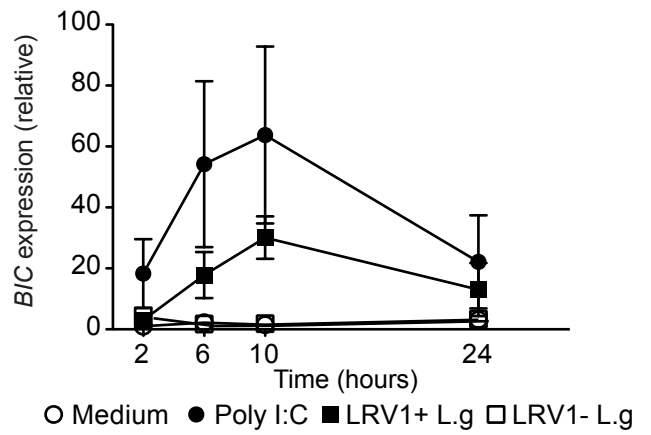
B



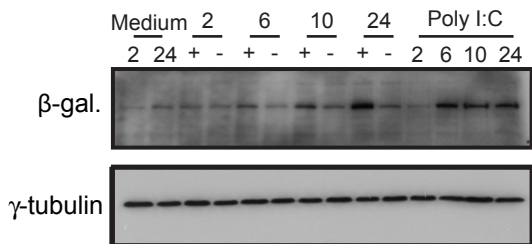
C



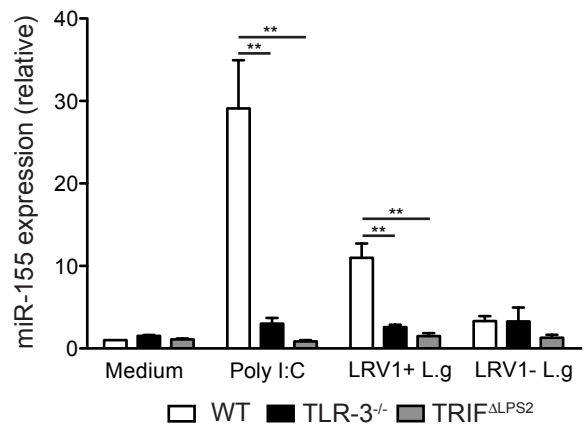
D



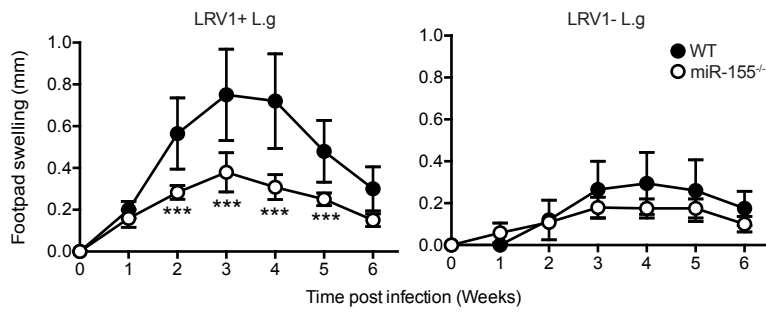
E



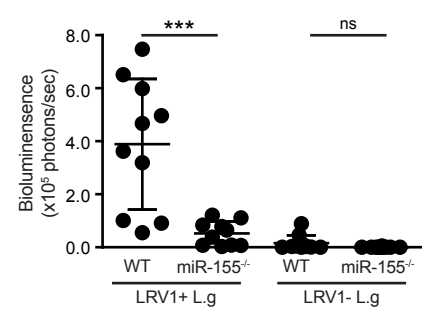
F



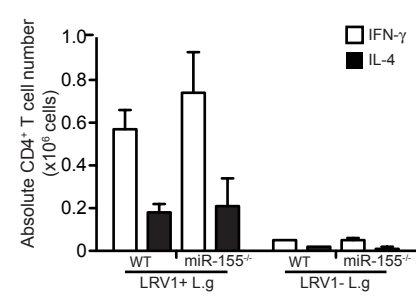
A



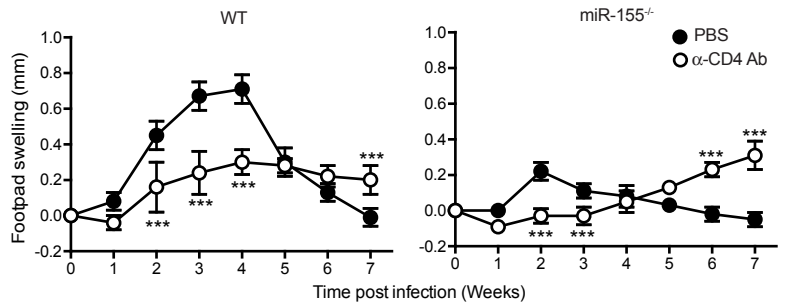
B



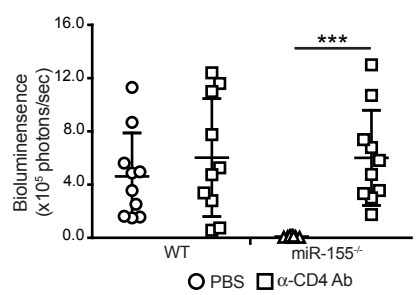
C



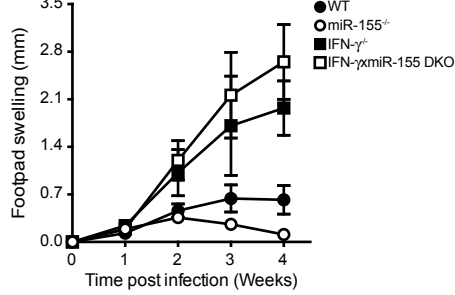
D



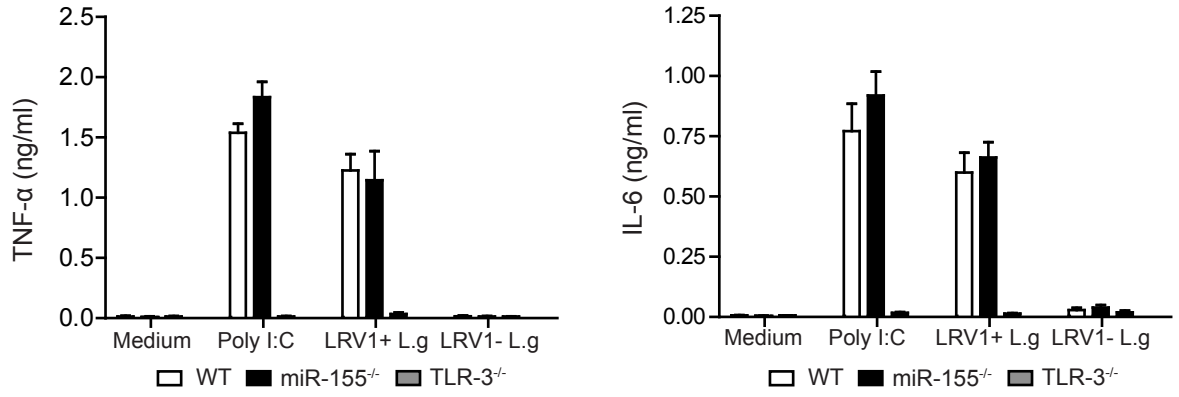
E



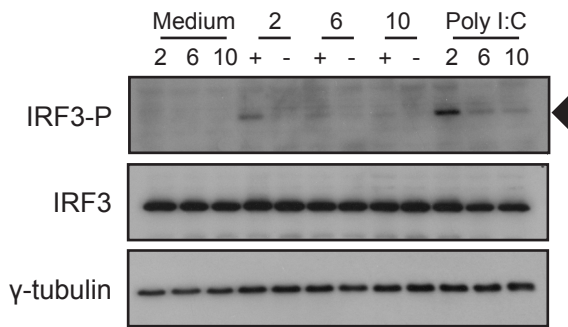
F



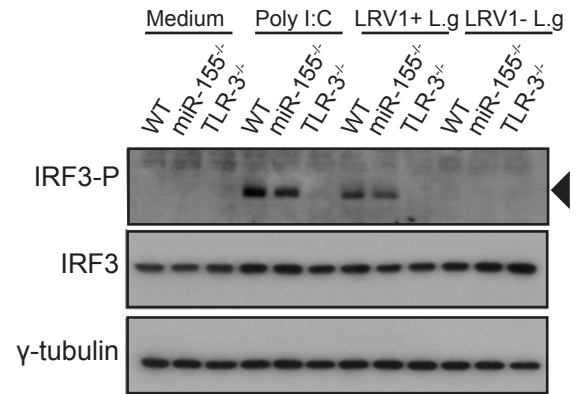
A



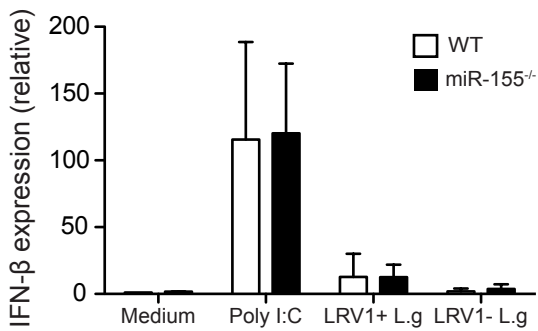
B



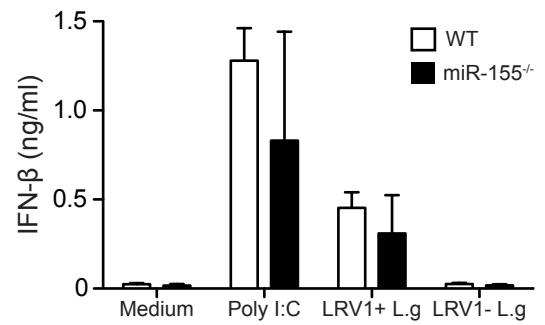
C



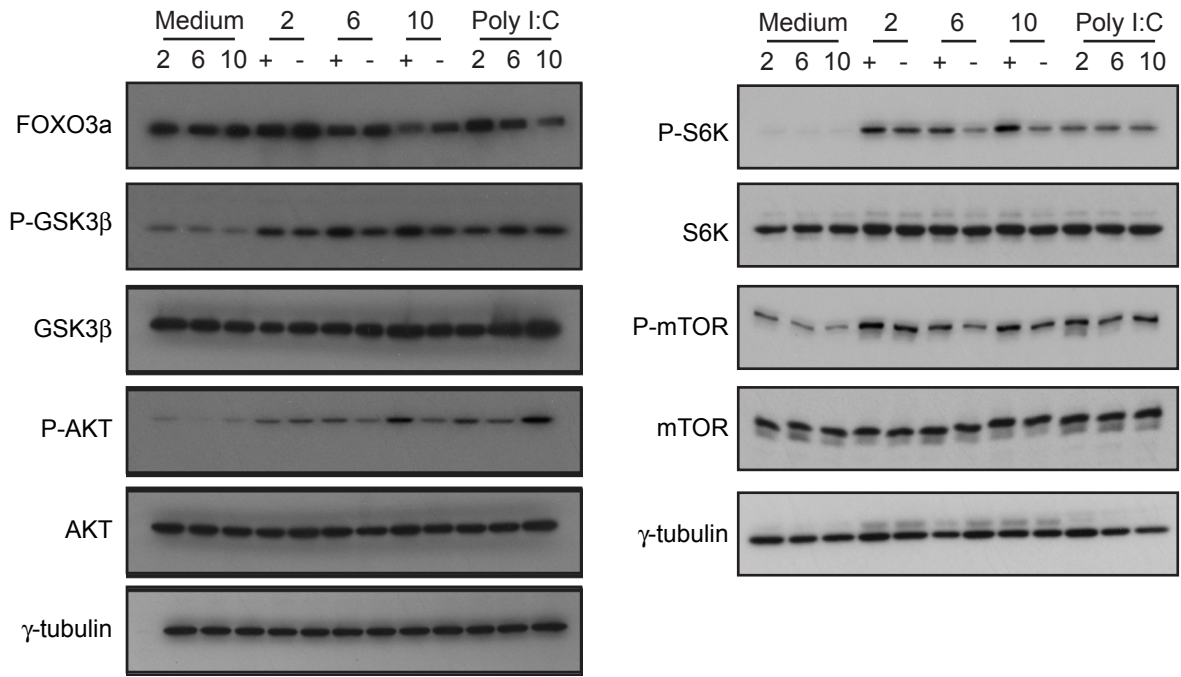
D



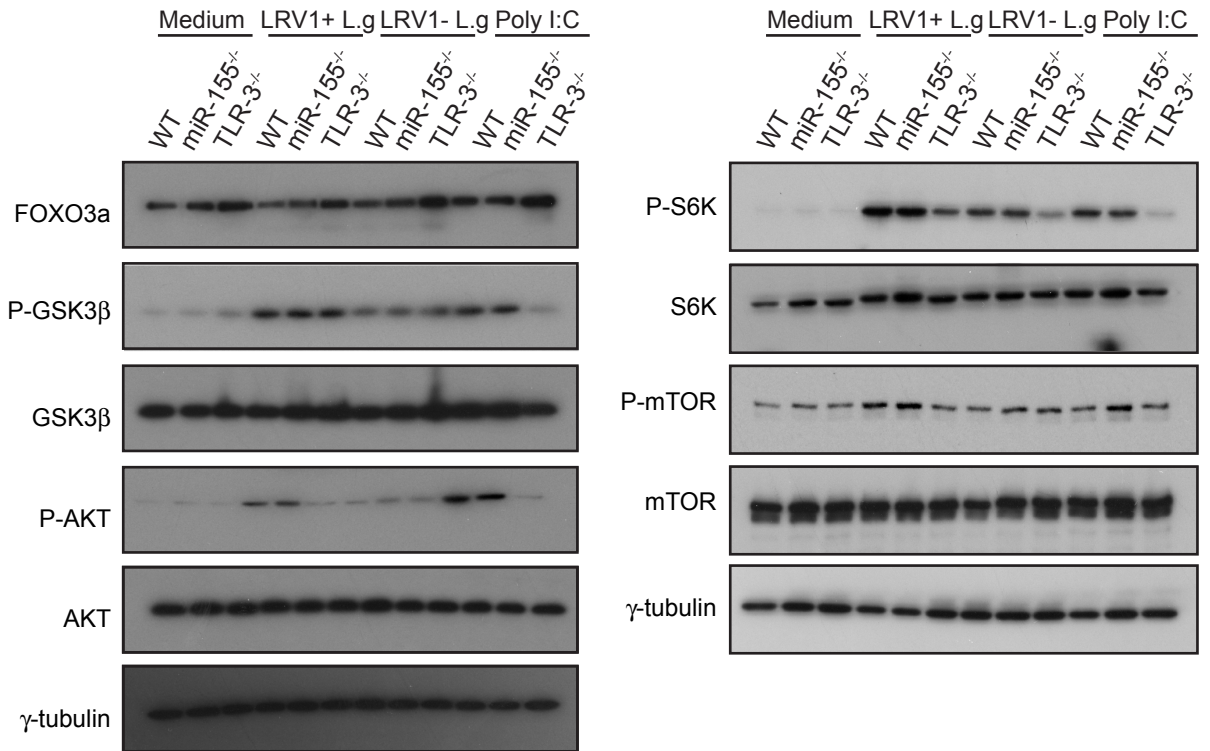
E



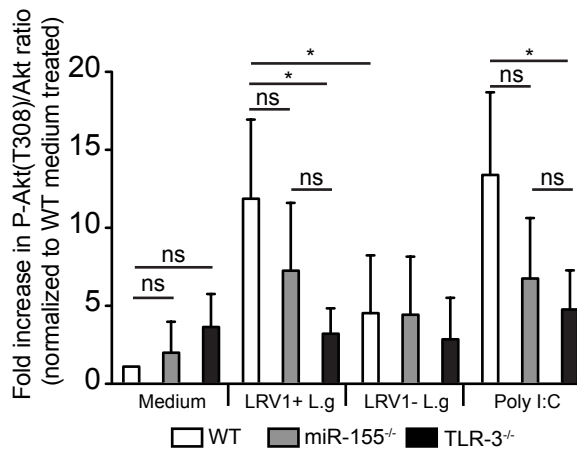
A



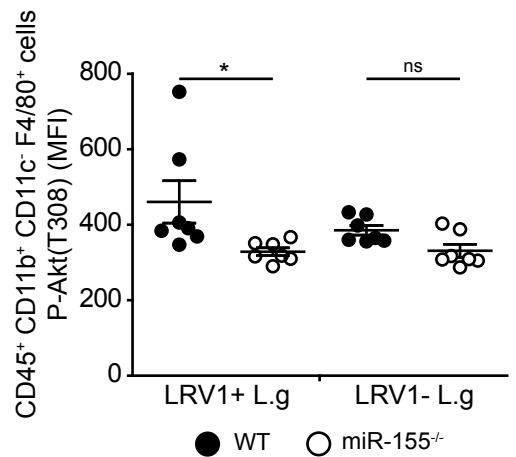
B



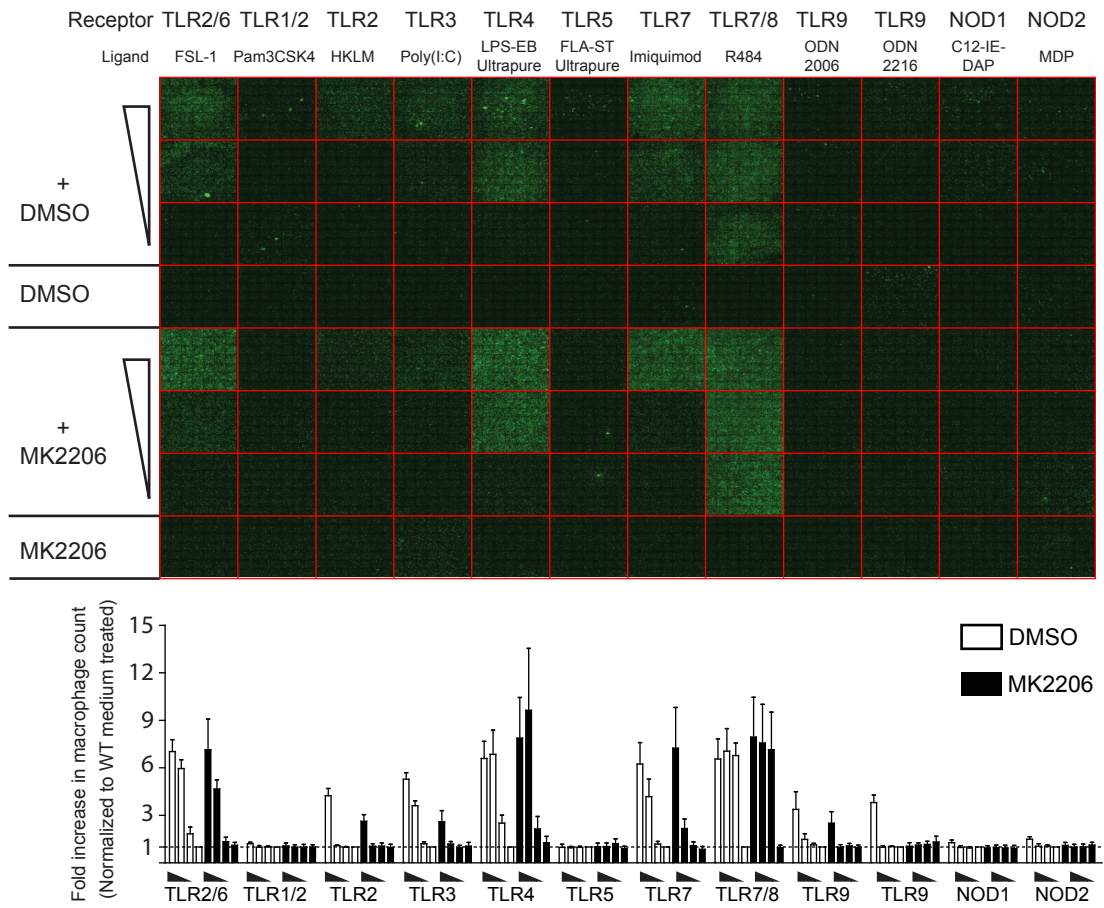
C



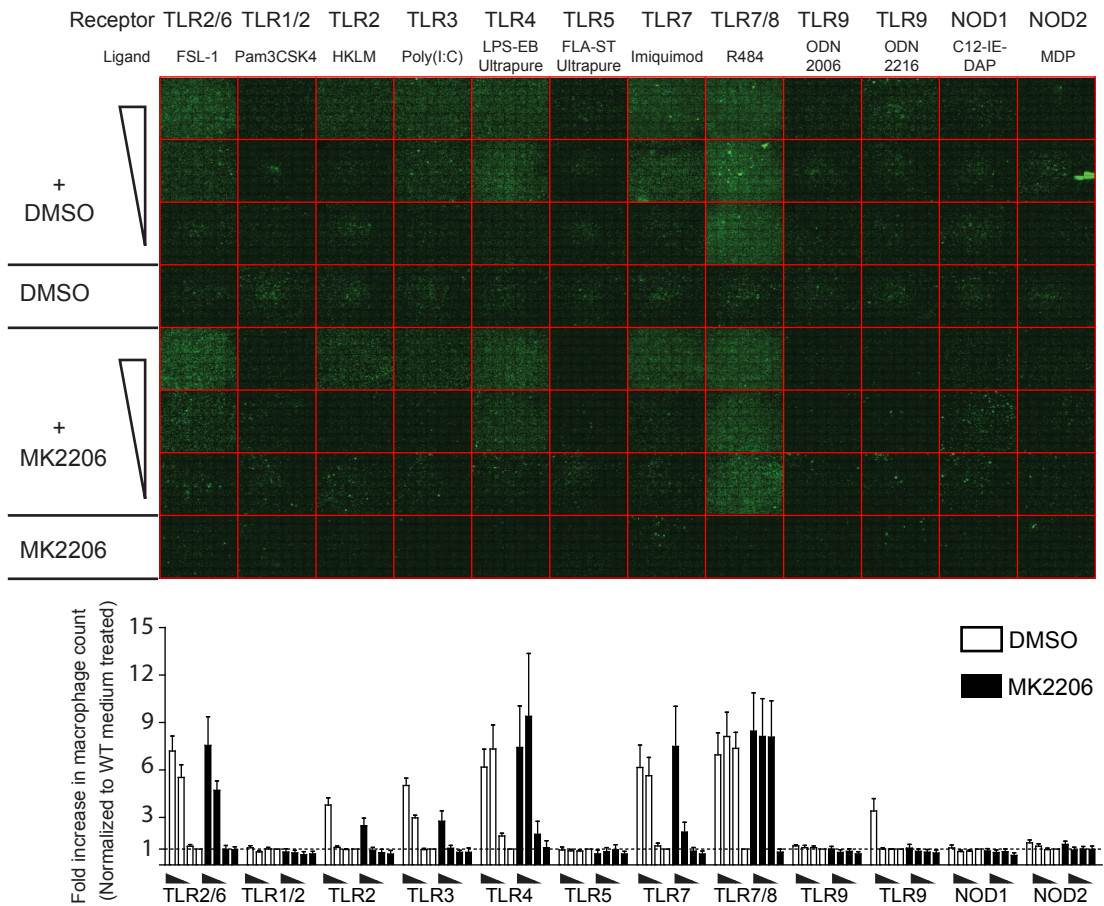
D



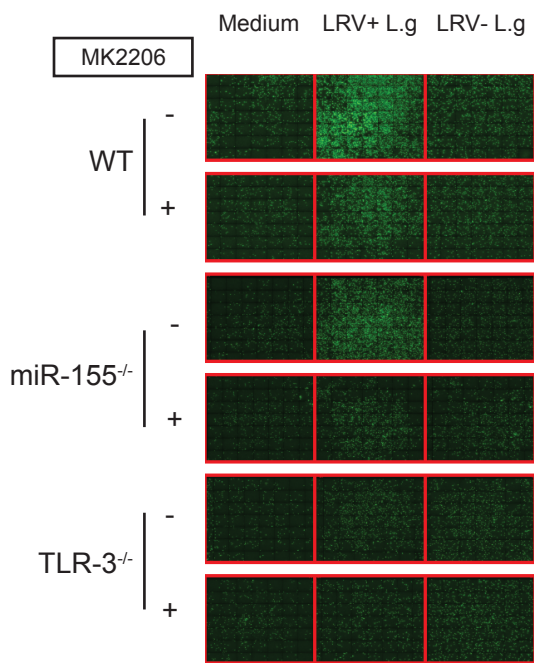
A



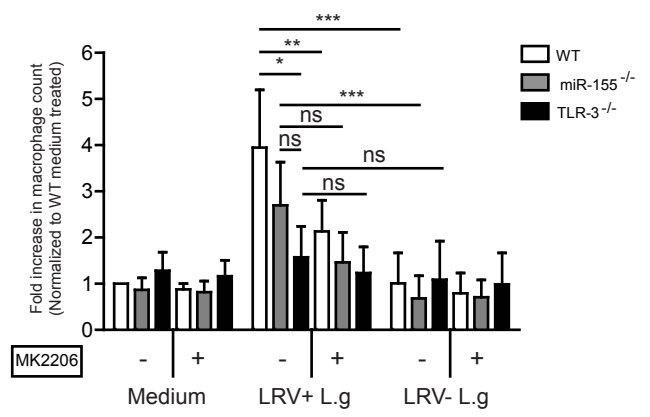
B



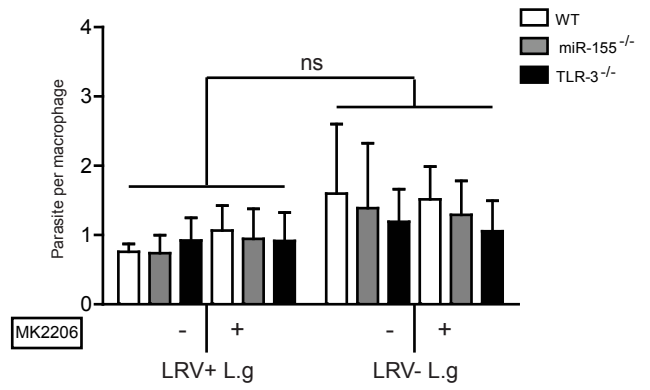
A

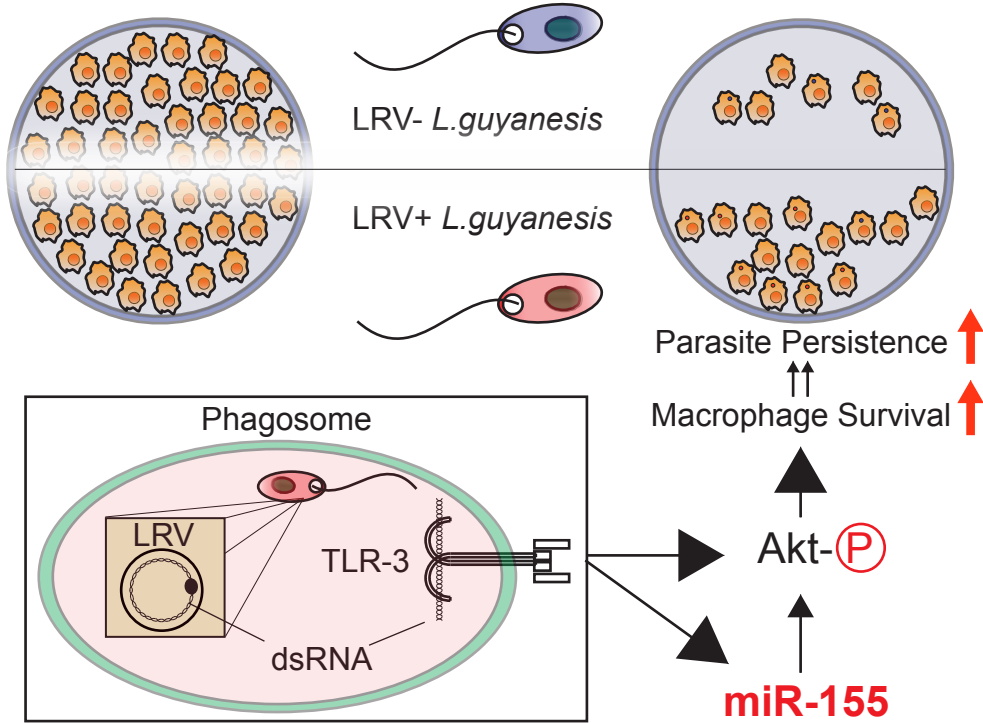


B

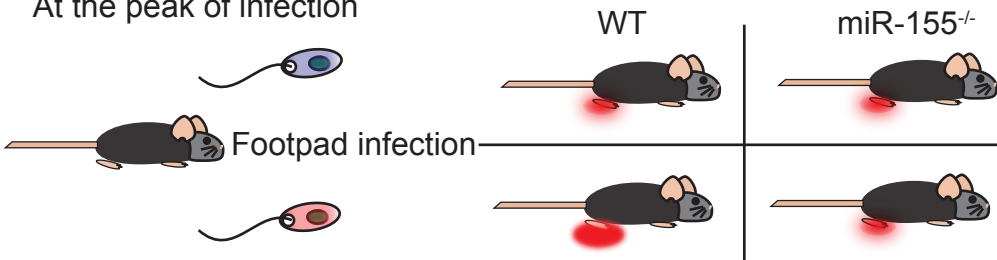


C





At the peak of infection



Highlights

- TLR-3 recognition of *Leishmania* RNA virus (LRV) induces miR-155 expression.
- MiR-155^{-/-} mice show decrease in the pathogenesis of LRV+ *Leishmania* infection.
- LRV induces the activation of PI3K/Akt signaling through TLR-3 and miR-155.
- LRV promotes parasite persistence by inducing host cell survival via Akt.

In Brief (eTOC blurb)

The viral endosymbiont of *Leishmania* parasites enhances virulence of its microbial host by promoting hyperinflammation through TLR-3. Eren et al. show an additional virulence mechanism wherein virus-containing *Leishmania* exploits innate receptor signaling pathways at a microRNA level, promoting macrophage survival and consequently parasite persistence through a TLR-3/miR-155/Akt signaling axis.

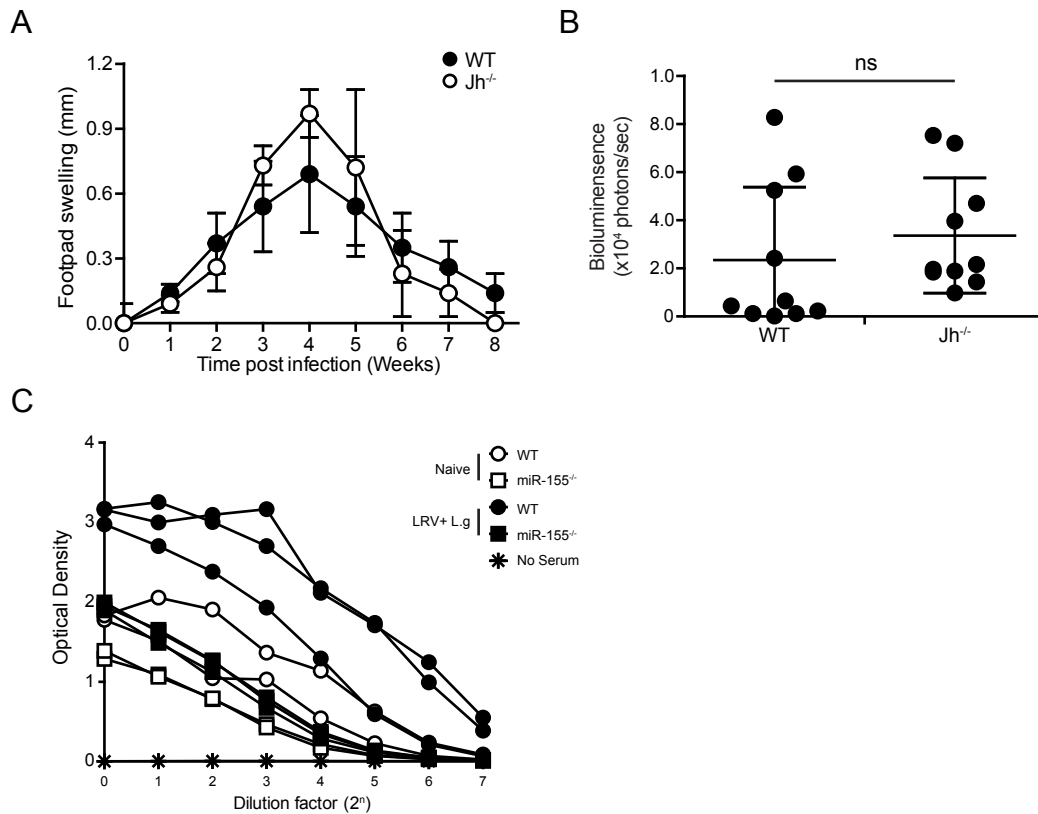


Figure S1, Related to Figure 2C. B cell responses does not affect LRV1-mediated disease progression.

(A-C) The hind footpads of mice were infected with 1.0×10^6 stationary LRV1+ L.g prosmatigotes.

(A) The footpad swelling of infected WT and Jh^{-/-} were monitored weekly during the course of infection. The graph is representative of two independent experiment.

(B) The parasite burden in 4-weeks infected WT and Jh^{-/-} were determined using relative luminescence.

(C) Total serum anti-LRV1 capsid IgG antibody titers of blood samples obtained from LRV1+ L.g infected (n=3) or naïve (n=2) WT and miR-155^{-/-} were measured using indirect ELISA against LRV1 capsid. Serums were diluted by two-fold serial dilutions in ELISA Diluent Solution (eBioscience®).

Data (A-B) are expressed as mean \pm SD and is representative of three (A) or two (B) independent experiment. Unpaired Student's t-test was used for evaluation of statistical significance. Not significant (ns).

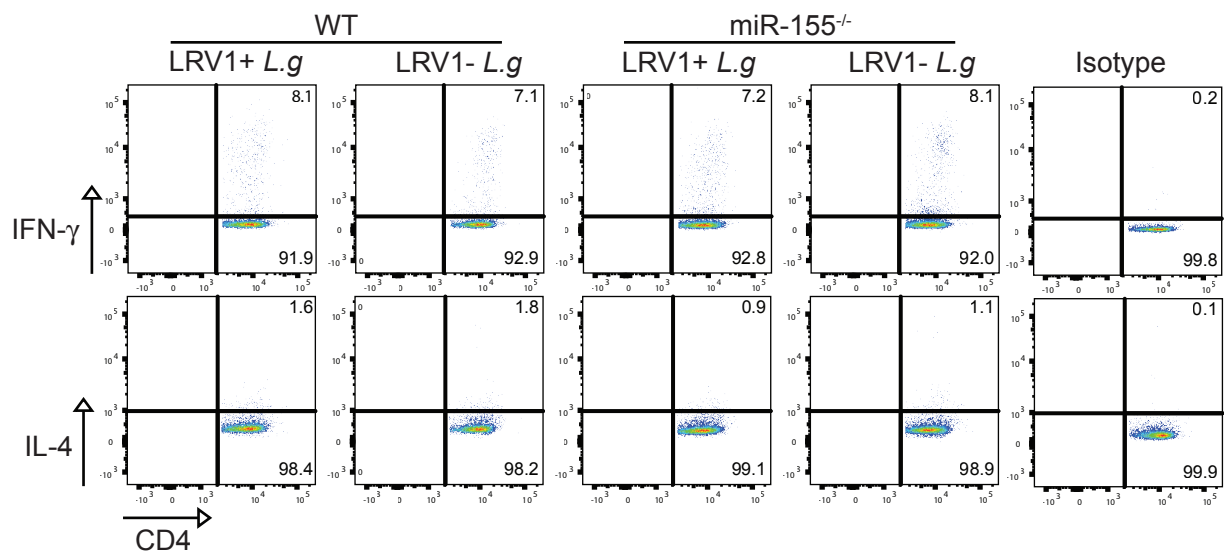


Figure S2, Related to Figure 2C. *L.guyanensis* infected WT and miR-155^{-/-} mice has similar levels of IL-4 and IFN-γ secreting CD4⁺ T cells at the peak of infection.

WT and miR-155^{-/-} mice were infected with 1.0×10^6 LRV1+ *L.g* or LRV1- *L.g* from the footpad. Popliteal lymph nodes were harvested at the peak of infection and dissociated to single cell suspension. Cells were stained for surface marker CD4 and for IFN-γ and IL-4 cytokines intracellularly. As a control, cells were stained with isotype-matched controls for IFN-γ or IL-4.

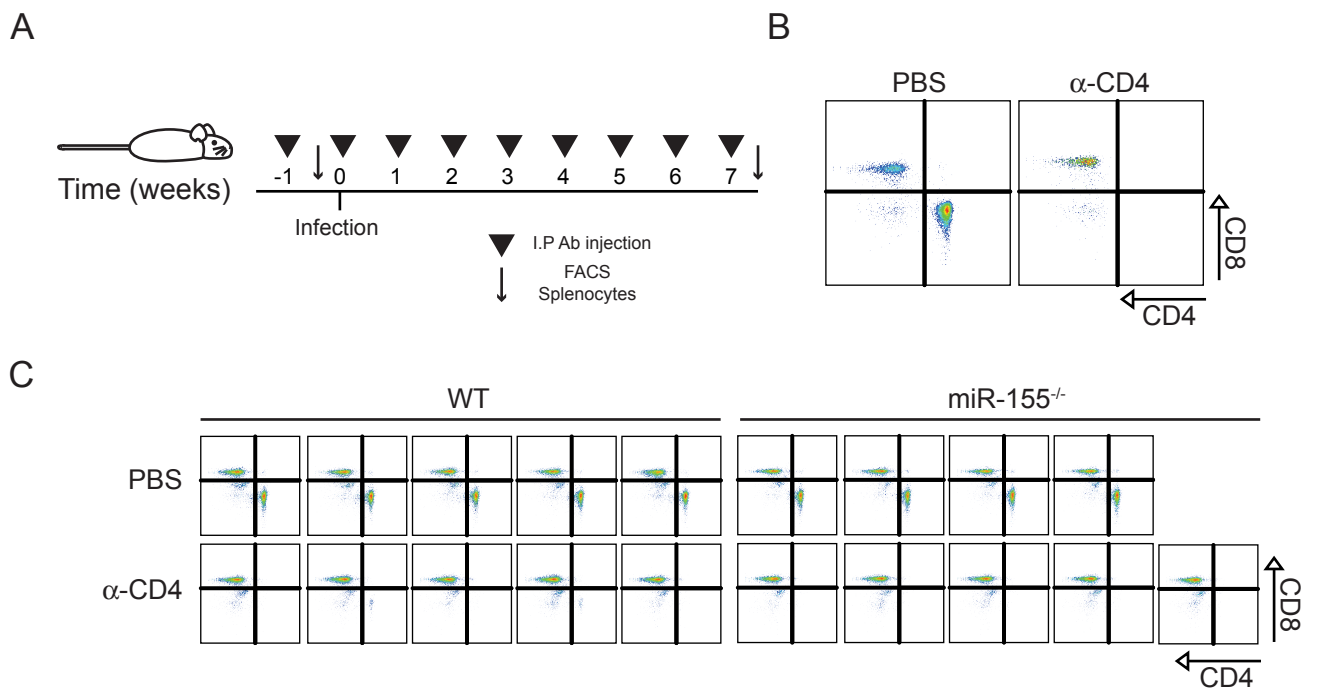


Figure S3, Related to Figures 2D and 2E. The FACS analysis of CD4 depleted mice splenocytes.

(A-C) WT and miR-155^{-/-} were treated with PBS or CD4 depleting antibody 5 days prior to LRV1+ L.g or LRV1- L.g infection and weekly afterwards (A). The flow cytometry analysis of splenocytes from treated mice at the day of infection (B) or at the end of the infection (C) for CD4 and CD8 T cell subsets was performed.

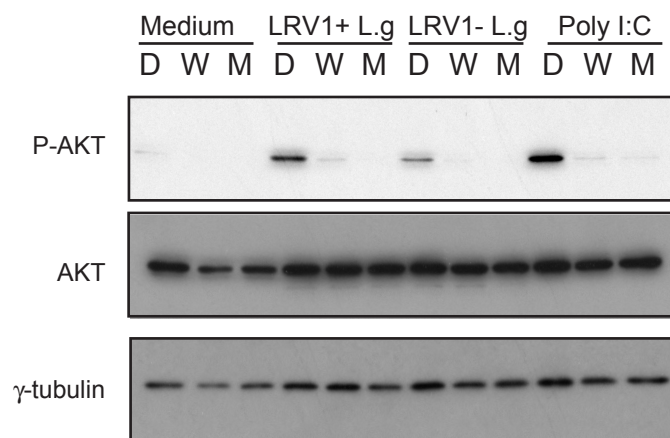


Figure S4, Related to Figure 4. The inhibition of PI3K diminishes LRV1+ L.g and poly(I:C)-mediated Akt activation.

WT macrophages were pre-treated with DMSO (D), 5 μ M MK-2206 (M) or 100nm Wortmanin (W) for 1 hour before the addition of indicated treatments. After 10 hours treatment, the protein levels of indicated proteins were assayed by immunoblotting. Representative blot were shown from three independent experiments.

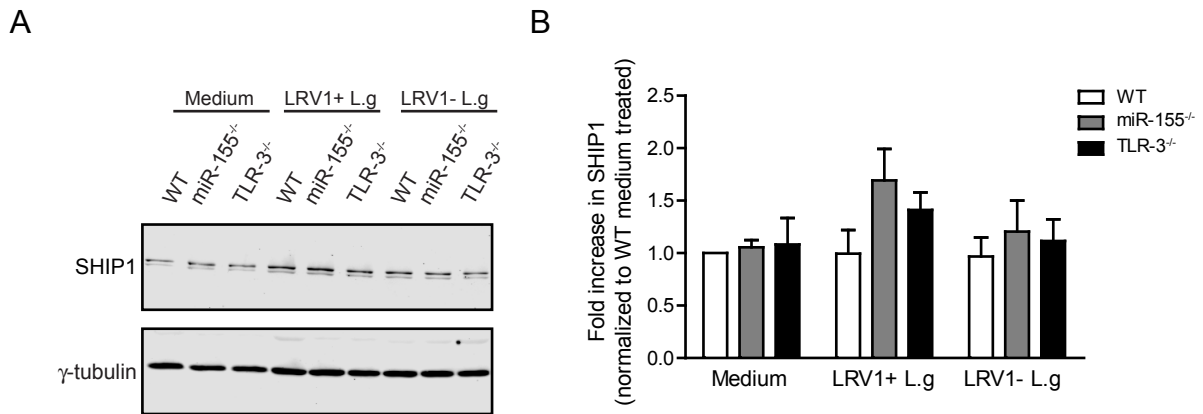


Figure S5, Related to Figure 4. Macrophages lacking miR-155 have increased amounts of SHIP1 protein in response to LRV1+ L.g infection.

(A-B) WT, miR-155^{-/-} and TLR-3^{-/-} macrophages were incubated with medium, LRV1+ L.g or LRV1- L.g for 24 hours. Cells were lysed and subjected to Western blot analysis to monitor the expression of SHIP1. Images were acquired and quantified using Licor Odyssey® CLx system.

(A) A representative blot is shown for SHIP1 expression.

(B) The blots were quantitated after being normalized to γ -tubulin, and fold-increase over WT medium treated is shown in bar graph. Data represents as mean \pm SD of three independent experiments performed in duplicate.

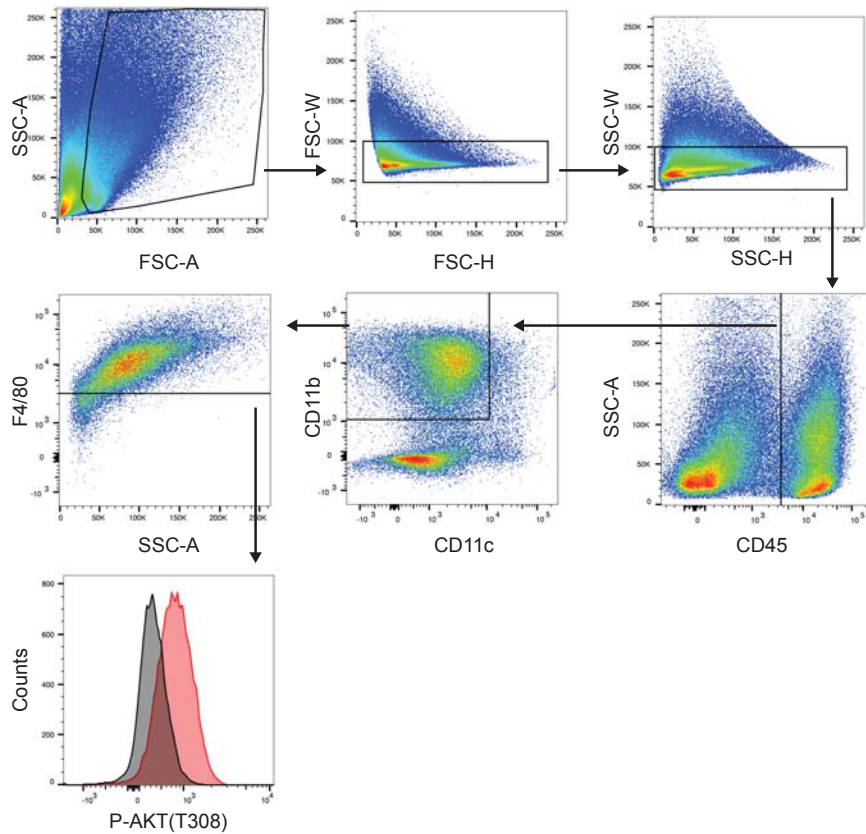


Figure S6, Related to Figure 4D. The gating strategy to measure phosphorylated-Akt in macrophage population in footpad lesion tissue of infected mice.

Footpad lesions harvested from mice infected 4 weeks with *Leishmania guyanensis* parasites were analyzed using flow-cytometry. The gating strategy is shown for the analysis of phosphorylated Akt at threonine 308 (p-Akt T308) residue in lesional macrophage population, as identified by expression of CD45, CD11b, CD11c and F4/80. Representative flow-cytometry histogram overlay of p-Akt (308) expression (red) and fluorescence-minus-one control (black) is shown for the indicated cell population.

| TLR2 /6 | TLR1/2 | TLR2 | TLR3 | TLR4 | TLR5 | TLR7 | TLR7/8 | TLR9 | TLR9 | NOD1 | NOD2 |
|------------------|------------------|-----------------|-----------------|-----------------|------------------|-----------------|-----------------|-----------------|-----------------|-----------------|-----------------|
| FSL1 | Pam3csk4 | HKLM | PolyI:C | LPS-EB | FLA-ST | R837 | R848 | ODN 2006 | ODN 2216 | C12-IE-DAP | MDP |
| ng/ml | ng/ml | Cells/ml | ng/ml | ng/ml | ng/ml | ng/ml | ng/ml | ng/ml | ng/ml | ng/ml | ng/ml |
| 10 ¹ | 10 ¹ | 10 ⁷ | 10 ³ | 10 ² | 10 ¹ | 10 ³ |
| 10 ⁰ | 10 ⁰ | 10 ⁶ | 10 ² | 10 ¹ | 10 ⁰ | 10 ² |
| 10 ⁻¹ | 10 ⁻¹ | 10 ⁵ | 10 ¹ | 10 ⁰ | 10 ⁻¹ | 10 ¹ |
| 0 | 0 | 0 | 0 | 0 | 0 | 0 | 0 | 0 | 0 | 0 | 0 |
| 10 ¹ | 10 ¹ | 10 ⁷ | 10 ³ | 10 ² | 10 ¹ | 10 ³ |
| 10 ⁰ | 10 ⁰ | 10 ⁶ | 10 ² | 10 ¹ | 10 ⁰ | 10 ² |
| 10 ⁻¹ | 10 ⁻¹ | 10 ⁵ | 10 ¹ | 10 ⁰ | 10 ⁻¹ | 10 ¹ |
| 0 | 0 | 0 | 0 | 0 | 0 | 0 | 0 | 0 | 0 | 0 | 0 |

Table S1, Related to Figure 5. Layout of multi-TLR array for high content microscopy.

The table displays the concentrations of pathogen-associated receptors (PRRs) cognate ligands that were used to stimulate macrophages in 96-wells high content imaging plates. The first three rows contain the information on PRRs, their cognate ligands, and units, respectively.

Supplemental Experimental Procedures

Measurement of total serum immunoglobulin G against LRV1 capsid

Plates (Nunc-Immuno™) were coated with LRV1 capsid protein at a concentration of 5µg/ml by incubating overnight at 4°C in 1xPBS. Plates were blocked with 1xAssay diluent (eBioscience) and incubated for 1 hour at room temperature. Blood samples were collected from mice under deep terminal anesthesia by cardiac puncture. Using these blood samples, a series of two-fold dilutions of serum in 1x Assay diluent (eBioscience) were prepared and incubated in coated/blocked plates for 2 hours at room temperature. The plates were incubated sequentially with biotin conjugated anti-mouse IgG (Jackson ImmunoResearch, USA) and streptavidin-conjugated HRP (eBioscience), followed by horseradish peroxidase (HRP)-substrate TMP. The colorimetric reaction was stopped by adding sulfuric acid and was detected at 450nm using a Synergy™ HT Multi-Mode Plate Reader (Biotek Instruments, Switzerland).

Technical details of animals

C57BL/6 mice were purchased from Harlan Laboratories (Netherlands). TLR3^{-/-} mice or miR-155^{-/-} mice were obtained from Prof. S. Akira (Osaka University, Japan) via P. Launois (WHO-IRTC, Lausanne, Switzerland) or Prof. Klaus Rajewsky (Max Delbrück Center for Molecular Medicine, Berlin, Germany) via Prof. Hans Acha-Orbea (UNIL, Lausanne, Switzerland). TRIF^{ΔLPS2} mice were obtained via B. Ryffel, (CNRS, Orléans, France). Jh^{-/-} mice and IFN-γ^{-/-} mice were obtained from Jackson Laboratories (United States). IFN-γxmiR-155 DKO mice were produced by intercrossing IFN-γ^{-/-} and miR-155^{-/-} mice. Mice were genotyped by PCR on tissue-isolated genomic DNA using the KAPA Mouse Genotyping Kit (KAPA Biosystems, USA). Mice were maintained under pathogen-free conditions at the animal facility of the Center of Immunity and Immunology, Lausanne (Switzerland). The mice and all experiments were performed under the guidelines set by the State Ethical Committee for the utilization of laboratory animals. All mice were backcrossed to C57BL/6 background for at least eight generations.

Primers used for mice genotyping

| | | | |
|------------------------|-------------------------------------|---|---|
| IFN-γ ^{-/-} | 5' - CCT TCT ATC GCC TTC TTG ACG-3' | 5' - AGA AGT AAG TGG AAG GGC CCA GAA G-3' | 5' - AGG GAA ACT GGG AGA GGA GAA ATA T-3' |
| miR-155 ^{-/-} | 5' - GTG CTG CAA ACC AGG AAG G-3' | 5' - CTG GTT GAA TCA TTG AAG ATG G-3' | 5' - CGG CAA ACG ACT GTC CTG GCC G-3' |

Technical details of MicroRNA microarray

The quality of RNA was checked using Agilent 2100 bioanalyzer and spectrophotometer. Agilent microRNA microarray 8x15K based on Sanger miRBase Release 18.0 was used. MicroRNA microarray was performed, acquired, and analysed by Lausanne Genomic Technology Facility (LTGF), University of Lausanne, Switzerland. Briefly, 100 ng RNA were hybridized after the labeling reaction with Cyanine-3 (Cy-3) using the miRNA Complete Labeling and Hyb Kit (Agilent Technologies), according to the manufacturer's instructions. The array was acquired using DNA microarray scanner (Agilent Technologies), and the raw data were

processed using Agilent Feature Extraction software (Version 10.7.3.1). The data were normalized and analyzed using R language software (Version 3.0.1); Bioconductor package preprocessCore Analysis and Bioconductor package limma. Moderated t-test was performed to compare the microRNA expression profile of macrophages infected with LRV1+ L.g to those with LRV1- L.g. P-values were adjusted with the Benjamini-Hochberg method, controlling for false discovery rate (FDR).

Technical details of the flow cytometry analysis

1x10⁶ cells in single cell suspension prepared from popliteal lymph nodes of infected mice were plated and stimulated with a cocktail containing PMA (50ng/ml), ionomycin (1µg/ml), and brefeldin A (100ng/ml) for 3 hours at 37°C. Prior to the staining procedure, cells were incubated with 2.4G2-conditioned medium to block CD16/32. Cells were first extracellularly stained for CD4 (Clone RM4.5 eBioscience®) and CD8 (Clone 53-6.7, Biolegend®), and were fixed and permeabilized using intracellular fixation and permeabilization buffer set according to the manufacturer's instructions (eBioscience). Cells were stained with IFN-γ (Clone XMG1.2 eBioscience) and IL-4 (Clone 11B11 eBioscience) or the matching Ig isotype antibodies.

Harvested footpad lesions from mice were cut into small pieces and treated with collagenase A (0.5 mg/ml; Boehringer-Mannheim, Mannheim, Germany) and DNase I (40 mg/mL; Boehringer-Mannheim) in DMEM medium supplemented with %5 FCS for 45 minutes at 37°C. Single cell suspension were prepared from samples using a dounce tissue grinder, and cell suspensions were filtered through a 40µM cell strainer. Cells were fixed in 1.5% paraformaldehyde in 1x PBS, pH 7.4 for 10 minutes and were permeabilized with methanol. Before staining, the samples were washed twice with 1xPBS, pH 7.4 supplemented with 1%BSA. Stainings were performed using CD45 (Clone 30-F11, eBioscience), CD11b (Clone M1/70, Biolegend), CD11c (Clone N418, Biolegend), F4/80 (Clone BM8, Biolegend) and p-Akt (T308) (Clone C31E5E, CST) in 1%BSA/1xPBS.

Technical details of the quantification of microRNA and mRNA using quantitative real time-PCR

Stem-loop RT-PCR was performed as previously described (Hurley et al., 2012). Briefly, total RNA was reverse transcribed using a specific stem-loop primer that anneals to 6 nucleotides of 3' miRNA. The abundance of product cDNA were measured by performing a RT-PCR reaction containing miRNA-specific forward primer, universal reverse primer, and locked-nucleic acid (LNA) based hydrolysis probe (Roche, UPL™ No.21, Switzerland).

Primers used for stem-loop RT-PCR

| | |
|--------------------------|---|
| MiR-155 stem loop primer | 5' - GTT GGC TCT GGT GCA GGG TCC GAG GTA TTC GCA CCA GAG CCA ACA CCC CTA T - 3' |
| MiR-155 forward primer | 5' - ACA CCA CGC ATT AAT GCT AAT TGT GAT -3' |
| MiR-16 stem-loop primer | 5' - GTT GGC TCT GGT GCA GGG TCC GAG GTA TTC GCA CCA GAG CCA ACC GCC AAT A - 3' |
| MiR-16 forward primer | 5' - ACA CAC GCA TAG CAG CAC GTA AAT AT -3' |
| Universal reverse primer | 5' - GTG CAG GGT CCG AGG T - 3' |

Total RNA was collected by RNazol® RT (Mrcgene). RNA was reverse-transcribed using the PrimeScript™ RT Reagent Kit with gDNA Eraser (Takara;Clontech Inc., USA). RT-PCR was performed on complementary DNA (cDNA) using following primers:

Primers used for RT-PCR

| Gene | Taqman® Catalog No. | Forward Primer | Reverse Primer |
|-------|---------------------|-------------------------------------|------------------------------------|
| IFN-β | Mm00439552_s1 | | |
| L32 | | 5'- AAG CGA AAC TGG CGG AAA C - 3' | 5'- TAA CCG ATG TTG GGC ATC AG -3' |
| BIC | | 5'- TTG GCC TCT GAC TGA CTC CT - 3' | 5'- GCA GGG TGA CTC TTG GAC TT -3' |

Data were acquired using LightCycler® 480 (Roche) and analyzed with the 2^{-ΔΔCt} method. Data were normalized to L32 expression and samples were calibrated to the expression of the gene of interest in medium-treated BMMs.

Technical details of Western blot analysis

Cells were lysed with lysis buffer after 2, 6 or 10 hours post-treatment. Cell lysis buffer was composed of 5x RIPA Buffer IV (Bio Basic Inc., Canada), 100x Protease/Phosphatase inhibitor cocktail (CST). Cell lysates were centrifuged at 13.000xg for 10 minutes. 4x Laemmli's Sample Buffer was added to the supernatant. Cells

lysates were size-fractionated by SDS-PAGE and wet-transferred to a nitrocellulose membrane. The membranes were blocked with 5% milk in Tris buffered saline with 0.1% tween-20 (TBST), and were incubated with primary antibody and with appropriate secondary antibody conjugated to HRP or IRDye® 800CW. The membranes were washed with TBST in between incubations. The immunoblot was revealed by the enhanced chemiluminescence Western blotting detection (GE Healthcare, UK) or with the Licor Odyssey® CLx system. The films (Amersham Hyperfilm™, GE Healthcare or SuperRX, Fuji, Japan) were developed using a radiograph (SRX-101a, Konica Minolta). Phosho-Akt (Thr308)/Akt ratio was quantified with densitometry analysis using Image J software.

Antibodies used for Western blots

| Name of Antigen | Source | Catalog No. |
|------------------------|----------------|-------------|
| Akt | CST | 4691 |
| Phosho-Akt (Thr308) | CST | 2965 |
| Foxo3a | CST | 2497 |
| GSK3-β | CST | 9315 |
| Phosho-GSK3-β (Ser9) | CST | 5558 |
| IRF-3 | CST | 4302 |
| Phosho-IRF-3 (Ser396) | CST | 4947 |
| m-TOR | CST | 2983 |
| Phosho-m-TOR (Ser2448) | CST | 5536 |
| p70 S6 kinase (S6K) | CST | 9202 |
| phosho-S6K (Thr389) | CST | 9234 |
| β-galactosidase | Promega® | Z3781 |
| γ-tubulin | Sigma-Aldrich® | T6557 |

Supplemental References

Hurley, J., Roberts, D., Bond, A., Keys, D., and Chen, C. (2012). Stem-loop RT-qPCR for microRNA expression profiling. *Methods Mol Biol* 822, 33-52.